Phosphorylation of Caveolin-1 on tyrosine-14 induced by ROS enhances palmitate-induced death of beta-pancreatic cells

Article *in* Biochimica et Biophysica Acta (BBA) - Molecular Basis of Disease · January 2015

DOI: 10.1016/j.bbadis.2014.12.021

CITATIONS
35

READS
424

9 authors, including:

Sergio Wehinger
Universidad de Talca
36 PUBLICATIONS **463** CITATIONS
SEE PROFILE

Rina J. Ortiz
Universidad Técnica Federico Santa María
25 PUBLICATIONS **464** CITATIONS
SEE PROFILE

Adam Aguirre
Yale University
46 PUBLICATIONS **1,109** CITATIONS
SEE PROFILE

Manuel Valenzuela-Valderrama
Universidad Central
53 PUBLICATIONS **1,032** CITATIONS
SEE PROFILE

Biochimica et Biophysica Acta 1852 (2015) 693–708

Contents lists available at ScienceDirect

Biochimica et Biophysica Acta

journal homepage: www.elsevier.com/locate/bbadis

Phosphorylation of caveolin-1 on tyrosine-14 induced by ROS enhances palmitate-induced death of beta-pancreatic cells

Sergio Wehinger [a,b], Rina Ortiz [a], María Inés Díaz [a], Adam Aguirre [a], Manuel Valenzuela [a], Paola Llanos [c], Christopher Mc Master [d,e], Lisette Leyton [a], Andrew F.G. Quest [a,*]

[a] Laboratory of Cellular Communication, Center for Molecular Studies of the Cell (CEMC), Advanced Center for Chronic Diseases (ACCDiS), Faculty of Medicine, Universidad de Chile, Santiago de Chile, Chile
[b] Research Program of Interdisciplinary Excellence in Healthy Aging (PIEI-ES), Faculty of Health Sciences, Department of Clinical Biochemistry and Immunohematology, Universidad de Talca, 3465548 Talca, Chile
[c] Institute for Research in Dental Sciences, Facultad de Odontología, Universidad de Chile, Santiago, Chile
[d] Departament of Pediatrics, Atlantic Research Centre, Dalhousie University, Halifax, NS, Canada
[e] Department of Biochemistry and Molecular Biology, Atlantic Research Centre, Dalhousie University, Halifax, NS, Canada

ARTICLE INFO

Article history:
Received 5 May 2014
Received in revised form 24 December 2014
Accepted 27 December 2014
Available online 5 January 2015

Keywords:
Caveolin-1
Palmitate
Reactive oxygen species
Tyrosine-14
Apoptosis
Beta cell

ABSTRACT

A considerable body of evidence exists implicating high levels of free saturated fatty acids in beta pancreatic cell death, although the molecular mechanisms and the signaling pathways involved have not been clearly defined. The membrane protein caveolin-1 has long been implicated in cell death, either by sensitizing to or directly inducing apoptosis and it is normally expressed in beta cells. Here, we tested whether the presence of caveolin-1 modulates free fatty acid-induced beta cell death by reexpressing this protein in MIN6 murine beta cells lacking caveolin-1. Incubation of MIN6 with palmitate, but not oleate, induced apoptotic cell death that was enhanced by the presence of caveolin-1. Moreover, palmitate induced de novo ceramide synthesis, loss of mitochondrial transmembrane potential and reactive oxygen species (ROS) formation in MIN6 cells. ROS generation promoted caveolin-1 phosphorylation on tyrosine-14 that was abrogated by the anti-oxidant N-acetylcysteine or the incubation with the Src-family kinase inhibitor, PP2 (4-amino-5-(4-chlorophenyl)-7(dimethylethyl)pyrazolo[3,4-d]pyrimidine). The expression of a non-phosphorylatable caveolin-1 tyrosine-14 to phenylalanine mutant failed to enhance palmitate-induced apoptosis while for MIN6 cells expressing the phospho-mimetic tyrosine-14 to glutamic acid mutant caveolin-1 palmitate sensitivity was comparable to that observed for MIN6 cells expressing wild type caveolin-1. Thus, caveolin-1 expression promotes palmitate-induced ROS-dependent apoptosis in MIN6 cells in a manner requiring Src family kinase mediated tyrosine-14 phosphorylation.

1. Introduction

Free fatty acids have been directly implicated in beta pancreatic cell dysfunction and death [1,2] and this has been suggested to contribute to beta cell death observed in type 2 diabetes mellitus (T2DM) [3–5]. Available evidence attributes the deleterious effects of lipotoxicity to increased levels in particular of saturated free fatty acids (FFAs), especially palmitate, rather than unsaturated FFAs, like oleate. Instead, unsaturated fatty acids are thought to protect against the deleterious effects of saturated FFAs [2,6,7], although the molecular mechanisms and the signaling pathways involved have not been clearly defined. A number of studies point towards reactive oxygen species (ROS) as being important mediators of lipotoxicity in beta cells [8–12]. Also, palmitate is a precursor for the de novo synthesis of ceramide, considered a lipid second messenger of cell death and implicated in lipotoxicity [13]. Thus, identifying important players normally expressed in beta cells that regulate these pro-apoptotic pathways is of considerable interest.

Caveolin-1 (CAV1) is a 178-amino acid member of a family of three proteins CAV1, CAV2 and CAV3 [14]. Two CAV1 isoforms exist, the full length version CAV1α, and a shorter CAV1β variant, which lacks the first 32 amino acid residues [15], including an important tyrosine phosphorylation site for Src family kinases [16,17]. CAV1 is present at many locations within the cell, including the plasma membrane, secretory vesicles, Golgi, mitochondria and the endoplasmic reticulum [18,19]. At the plasma membrane, CAV1 is associated with microdomains termed “lipid rafts” and membrane invaginations called “caveolae”, both of which are membrane structures, rich in cholesterol and sphingolipids, important for vesicle trafficking and signal transduction [20].

* Corresponding author at: Laboratory of Cellular Communication, Center for Molecular Studies of the Cell (CEMC), Advanced Center for Chronic Diseases (ACCDiS), Facultad de Medicina, Universidad de Chile, Av. Independencia 1027, Santiago, Chile. Tel./fax: +56 2 7382015.
E-mail address: aquest@med.uchile.cl (A.F.G. Quest).

http://dx.doi.org/10.1016/j.bbadis.2014.12.021
0925-4439/

CAV1 has long been implicated in cell death, either by sensitizing to or directly inducing apoptosis. Specifically, CAV1 is known to regulate the cell cycle [21] and cellular senescence [22], to act as a tumor suppressor [18,23] and function as a modulator of cell death [24]. A variety of signaling pathways have been linked to such functions of CAV1, including mitochondrial permeabilization, caspase activation and inhibition of pro-survival mechanisms, including Ras/Raf/ERK, PI3K/Akt and Wnt/β-catenin signaling pathways [25–27]. Nonetheless, pro-survival effects of CAV1 have also been reported (reviewed in [24]), suggesting that the relationship between CAV1 and cell fate is complex and context-dependent.

The CAV1α isoform is phosphorylated on tyrosine-14 by the Src family tyrosine kinases Src, Abl or Fyn [16,17,28]. This phosphorylation has been observed in response to oxidative stress and is also suggested to represent a marker for stress [29–31] associated with enhanced sensitivity to cell death [32,33]. Accordingly, CAV1 expression has previously been associated with sensitivity to different apoptosis-inducing cytotoxic stimuli [34–37]. Although CAV1 is normally present in beta cells [38] where it participates in the regulation of insulin secretion [38,39], no study to date has associated CAV1 expression with enhanced sensitivity to lipotoxicity in beta cells. Here, we investigated the role of CAV1 in palmitate-induced cell death in the murine MIN6 beta cell model. We provide evidence indicating that palmitate exposure enhances ceramide synthesis, ROS generation and mitochondrial damage, which together favor beta cell apoptosis in a manner that is enhanced by phosphorylation of CAV1 on tyrosine-14.

2. Materials and methods

2.1. Materials

Dulbecco's Modified Eagle's Medium (DMEM), 2-mercaptoethanol, HEPES, and trypsin-EDTA were from GIBCO (Invitrogen, Carlsbad, CA). Fetal calf serum was from Biological Industries (Kibbutz Beit Haemek, Israel) and Isopropyl β-D-1-thiogalactopyranoside (IPTG) from US Biological (Swampscott, MA). Propidium iodide (PI), fatty acid-free bovine serum albumin (BSA), sodium palmitate, oleic acid, tiron, trolox, Oil Red O, rhodamine, dihydrorhodamine, myriocin, fumonisin B1, sodium fluoride, NP-40 (Igepal CA-630), leupeptin, antipain, benzamidine, PMSF (phenylmethylsulfonyl fluoride) and Na_3VO_4 (sodium orthovanadate) were purchased from Sigma-Aldrich (St. Louis, MO). C2-ceramide, C2-dihydroceramide and the Src inhibitor PP2 ((4-amino-5-(4-chlorophenyl)-7(dimethylethyl)pyrazolo[3,4-d]pyrimidine)) were from Enzo life Sciences International (Plymouth Meeting, PA). NAC (N-acetyl cysteine) was from Merck (Darmstadt, Germany). The transfection reagent Superfect and plasmid extraction kit were from Qiagen (Valencia, CA). The transfection reagent Fugene was from Roche Diagnostics. Rabbit polyclonal antibodies anti-caveolin-1 (Transduction Laboratories, Lexington, KY) and anti-actin (R&D Systems, Minneapolis, MN) as well as the mouse monoclonal antibodies anti-pY14-caveolin-1 (Transduction Laboratories, Lexington, KY), anti-caveolin-1 (Transduction Laboratories, Lexington, KY), goat anti-rabbit, goat anti-mouse and donkey anti-guinea pig IgG antibodies coupled to horseradish peroxidase (HRP) were from Bio-Rad Laboratories (Hercules, CA), Sigma-Aldrich (St. Louis, MO) and Jackson ImmunoResearch (West Grove, PA), respectively. The EZ-ECL chemiluminescent substrate was from Biological Industries (Kibbutz Beit, Haemek, Israel) and the BCA protein determination kit was from Pierce (Rockford, IL).

2.2. Cell culture

MIN6 cells were cultured in DMEM High (4.5 g glucose/l) supplemented with 10% fetal calf serum, antibiotics (10,000 U/ml penicillin, 10 μg/ml streptomycin) and 50 μmol/l of 2-mercaptoethanol at 37 °C in humidified 5% CO_2. For all experiments evaluating the effect of fatty acid exposure, MIN6 cells were serum-deprived for 12 h and incubated in medium without 2-mercaptoethanol. B16F10 cell line, a mouse melanoma cell line (ATCC, #CRL6475), was used as a negative control for insulin expression in western blot assays. B16F10 were maintained in RPMI 1640 medium supplemented with 10% FBS and antibiotics.

2.3. Stable transfection of MIN6 cells

The plasmids pLacIOP and pLacIOP-caveolin-1 used here were previously described [40]. MIN6 cells were grown to 60–80% confluence in 10 cm plates and then incubated with the transfection reagents Superfect or Fugene, following the manufacturer's instructions. After 24 h, cells were plated in DMEM high glucose with 10% serum, containing hygromycin (750 μg/ml) and cultured for 3 weeks to yield stably transfected MIN6 (Mock) and MIN6 (Cav-1) cells.

2.4. Animals

Male C57BL/6J mice (8–12 weeks old) were obtained from the Animal Facility at the Faculty of Medicine, Universidad de Chile. Room temperature was kept constant at 21 °C, and light was maintained on a 12:12 h light–dark cycle, with free access to food and water. The Bioethics Committee for Animal Research, Faculty of Medicine, Universidad de Chile, approved all experimental protocols used in this work.

2.5. Mice pancreatic islet isolation

The pancreas extracted from male mice was digested with liberase to isolate the islets of Langerhans as previously described [41]. Islets were picked by hand under a dissecting microscope, and rinsed three times in Hank's solution.

2.6. Immunofluorescence staining

The paraffin-embedded tissues were processed and incubated with anti-insulin (1/200) and anti-caveolin-1 antibodies (1/200). Anti-guinea pig FITC and Alexa Fluor 546 anti-rabbit IgG were used as secondary antibodies (1/200). The cross sections of pancreatic tissue were 5 μm thick.

2.7. Site directed mutagenesis of CAV1

The Y14F and Y14E mutations were introduced by double PCR, using the primers 5′-cct ctt tac cgt tcc cat cc-3′ (sense) and 5′-gaa cgg taa aga ggt gcc c-3′ (antisense) and 5′-ggg cac ctc gag acc gtt ccc-3′ (sense) and 5′-cat ggg aac ggt ctc gag gtg-3′ (antisense), respectively. The design of primers includes the sequence overlapping the region containing the tyrosine-14 codon. External primers used to amplify the full-length CAV1 sequence were: 5′-ccg agc gcg gcc gcc atg tct ggg ggc aaa tac-3′ (sense) and 5′-tat ctg gcg gcc gct tat gtt tct ttc tgc atg ttg-3′ (antisense), both harboring *Not*I sites. The final PCR product from a double PCR reaction was then cloned into pPCR-Script amp+. Positive colonies were identified and sequenced in both directions. The CAV1-encoding sequence with the Y14F and Y14E mutations was sub-cloned from pPCR-Script amp+ into the multiple cloning site of pLacIOP, following digestion with *Not*I. Correct orientation of the insert was determined by PCR using an external anti-sense primer targeting the vector (5′-ttg tct cct tcc gtg ttt ca-3′) in combination with the sense primer used to generate the Y14F and Y14E mutations.

2.8. Fatty acid solutions

To expose MIN6 cells to the fatty acids palmitate and oleate, these fatty acids were prepared in stock solutions containing 1800 mmol/l of palmitate or oleate in 90% ethanol. These solutions were incubated at 70 °C for 30 min vortexing repetitively during this period and then

diluted to 20 mmol/l in 5.5% fatty acid-free BSA dissolved in PBS and sterilized by filtration through a 0.22 μm Millipore filter. These solutions were stored at −20 °C until utilization in experiments. Aliquots were only thawed once. As a control, a "vehicle solution" with BSA alone was prepared by diluting a 90% ethanol solution 90× in 5.5% fatty acid-free BSA dissolved in PBS.

2.9. Annexin V binding assay

Free fatty acid-induced apoptosis was evaluated by flow cytometry (BD FACSCanto instrument) using the Annexin V–Propidium iodide Apoptosis Detection Kit No. 1 (BD Pharmingen).

2.10. Viability assays with propidium iodide

Cell viability was generally analyzed using a simple flow cytometry procedure, as previously described [42,43]. In this assay, after setting the baseline to exclude cell debris, cells impermeable to PI (10 μg/ml) were considered as viable and two populations of PI-permeable cells were distinguished, based on fluorescence intensity: apoptotic cells, with hypodiploid DNA content, and necrotic cells, with intact DNA. The window utilized to define normal DNA content was obtained using cells permeabilized with methanol and stained with PI. To assess the viability in the presence of free fatty acids, C2-ceramide or hydrogen peroxide, MIN6 cells were serum-starved for 12 h and then incubated with either vehicle solution alone or in the presence of increasing concentration solutions for 16 h (C2-ceramide or hydrogen peroxide) or 24 h (palmitate or oleate). For de novo ceramide synthesis inhibition experiments, transfected MIN6 cells were pre-incubated for 1 h with fumonisin B1 (50 μM) or myriocin (100 nM) and then, free fatty acids were added. Similarly, for viability assays with anti-oxidants, MIN6 cells were pre-incubated with NAC (3 mM), for 1 h and then incubated with (B) palmitate (2 mM) or with (C) C2-ceramide (200 μM) for 24 h and viability was evaluated by flow cytometry following PI staining, as indicated. Finally, to assess viability in the presence of PP2, MIN6 cells were pre-incubated with the Src-family kinase inhibitor PP2 (10 μM) for 1 h, incubated with palmitate for 24 h, stained with PI and evaluated by flow cytometry.

2.11. Caspase 3 activity assay

Caspase activity in cell lysates was determined by quantifying DEVDase activity in MIN6 cells exposed to free fatty acids. Cells were lysed in HEPES 250 mM, pH 7.4, 25 mM CHAPS and 25 mM DTT and DEVDase activity was determined by the release of the fluorescent dye 7-amino-4-trifluoromethylcoumarin (AFC) from the caspase-3 substrate Asp-Glu-Val-Asp-AFC (Enzo Life Sciences) in a Synergy Neo Multi-Mode plate reader (Biotek). A unit of enzymatic activity was defined as 1 μmol of substrate transformed per minute, per mg protein extract [44].

2.12. Western blotting

Cells grown to 80% confluence were washed twice with cold PBS and lysed in 0.2 mM HEPES (pH 7.4) buffer containing 0.1% SDS, phosphatase inhibitors (1 mM Na_3VO_4), as well as a protease inhibitor cocktail (10 mg/ml benzamidine, 2 mg/ml antipain, 1 mg/ml leupeptin, 1 mM PMSF). Protein concentration was determined using the BCA assay. Total protein extracts (30 μg/lane) were separated by SDS-polyacrylamide gel electrophoresis (SDS-PAGE). Separated proteins were then transferred to nitrocellulose membrane. Blots were blocked with 5% milk in 0.1% Tween–PBS and then probed with anti-actin (1:5000), anti-caveolin-1 (1:5000) or anti-insulin (1:5000) polyclonal antibodies or blocked with 5% Gelatin in 0.1% Tween–PBS for incubations with anti-pY14-caveolin-1 (1:3000) monoclonal antibody. Bound antibodies were detected with HRP-conjugated secondary antibodies and the EZ-ECL system.

2.13. Ceramide levels

The ceramide levels from stably transfected MIN6 were determined using the diacylglycerol assay. Briefly, MIN6 cells were incubated with free fatty acids for 16 h and then lipids were extracted as previously described [45]. These extracts were prepared for the determination of ceramide by the diacylglycerol kinase assay [46] using brain ceramide (Avanti Polar Lipids, Alabaster, AL) as a standard. In this assay, lipid extracts were incubated with *Escherichia coli* 1,2-diacylglycerol kinase (DAG kinase) in the presence of gamma ^{32}P-ATP (100,000 cpm/nmol, Sigma-Aldrich) at 25 °C for 30 min. This reaction that converts ceramide to ^{32}P ceramide-phosphate was terminated by the addition of 0.5 ml ice-cold chloroform–methanol (1:2 vol/vol). The lipids were extracted with 0.5 ml chloroform and 0.5 ml 1 mM NaCl, centrifuged at 14,000 ×*g* for 3 min and the upper aqueous phase was discarded. The lower organic phase was washed sequentially with 1% perchloric acid, 0.3 ml chloroform–methanol (1:2 vol/vol), 0.2 ml chloroform and 0.2 ml of water. The organic phase was dried under N_2 and resuspended in chloroform–methanol (95:5 vol/vol), spotted onto silica Gel 60 TCL plates, and developed in a solvent mixture of chloroform–acetone–methanol–acetic acid–water (10:4:3:2:1 vol/vol). The TCL plates were revealed with photographic film to identify the radioactive bands that were then scraped into vials containing liquid scintillation fluid and radioactivity of the samples was quantified in a scintillation counter (Beckman Coulter LS 5000TA, Mississauga, ON, Canada). The radioactivity was normalized to the total amount of phosphorus in samples as previously described [47].

2.14. Flow cytometry assay for ROS production

Dihydrorhodamine 123 (DHR-123, 1 μM), a fluorescence probe that is sensitive to oxidative stress, was added to cell suspensions 30 min prior to completing the experiment. After the indicated periods of free fatty acid, or C2-ceramide exposure, cells were washed with PBS to remove excess probe. The fluorescence of cells was analyzed by flow cytometry as described [42].

2.15. Analysis of mitochondrial transmembrane potential

To detect changes in transmembrane mitochondrial potential, the cationic voltage-sensitive probe rhodamine 123 was used. This probe reversibly accumulates in the mitochondria [48]. Stably transfected MIN6 cells were incubated with palmitate (2 mM), oleate (2 mM), C2-ceramide (200 μM) or DH-C2-ceramide (200 μM) for 4 h as indicated in the figure legends. Cells were labeled with 1 μM (final concentration) of rhodamine 123 at 37 °C in cell medium for 1 h before terminating the experiment. After washing with ice cold PBS, the samples were analyzed by flow cytometry using excitation and emission wavelengths of 500 and 536 nm, respectively. The results were expressed as histogram profiles showing two cell populations. Reduced fluorescence levels are indicative of cells with decreased mitochondrial membrane potential.

2.16. Src family kinase inhibition assays

To inhibit CAV1 phosphorylation on tyrosine-14, MIN6 cells were pre-incubated with the Src-family kinase inhibitor PP2 (10 μM), a concentration known to lead to significant inhibition of pSrc-Y416 [49–51], before incubation with either H_2O_2 (positive control), vehicle alone (negative control) or with palmitate (2 mM), oleate (2 mM) or C2-ceramide (200 μM) for 4 h. Then, the levels of CAV1 phosphorylated on tyrosine-14, CAV1 and β-actin were evaluated by western blotting.

2.17. Nuclear fragmentation assay

Confluent MIN6 cell monolayers were grown on 12 mm-glass coverslips in 24-well plates, serum deprived and then exposed to palmitate or

oleate for 24 h, fixed with 4% paraformaldehyde in 100 mM PIPES buffer pH 6.8, containing 40 mM KOH, 2 mM EGTA and 2 mM $MgCl_2$ for 30 min. Cells were then washed three times with washing solution (50 mM Tris buffer pH 7.6 containing 0.15 NaCl and 0.1% sodium azide) and permeabilized with 0.1% Triton X-100 for 10 min. To identify the nuclei, cells were stained with PI (10 μg/ml) for 5 min. Coverslips were washed and mounted on microscope slides with 10% Mowiol-2.5% 1,4-Diazabicyclo [2.2.2] octane and samples were visualized by fluorescence microscopy (LSM Microsystems Pascal 5 confocal microscope, Carl Zeiss, Thornwood, NY) upon excitation at 543 mm using a 570 nm emission filter. The nuclei that were reduced in size and/or fragmented were interpreted as representing apoptotic nuclei.

2.18. Lipid droplets

To visualize intracellular lipid inclusions called "lipid droplets", MIN6 cells were incubated in 24-well plates with palmitate or oleate (1 or 2 mM) for 16 h and then washed with PBS, fixed with 60% isopropanol for 5 min and then stained with Oil Red O reagent, as described previously [52]. In brief, coverslips were incubated with 0.22% Oil Red O solution for 10 min at room temperature. Coverslips were then washed four times and stained with hematoxylin to visualize the cells and mounted on microscope slides with 10% Mowiol-2.5% 1,4-Diazabicyclo [2.2.2] octane. The stained cells were observed and recorded photographically. Lipid droplets observed were quantified using the Image J1.40 software (Wayne Rasband National Institutes of Health, USA) by calculating the percentage of lipid droplet area compared to the total cell area.

2.19. Statistical analysis

Results were compared statistically assuming non-parametric distribution. For paired data, the Wilcoxon test was used. For unpaired data, the Mann–Whitney test was employed. Also, for time-course experiments, 2-Way ANOVA with post-hoc multiple comparison analysis was employed. The method employed for analysis is specifically

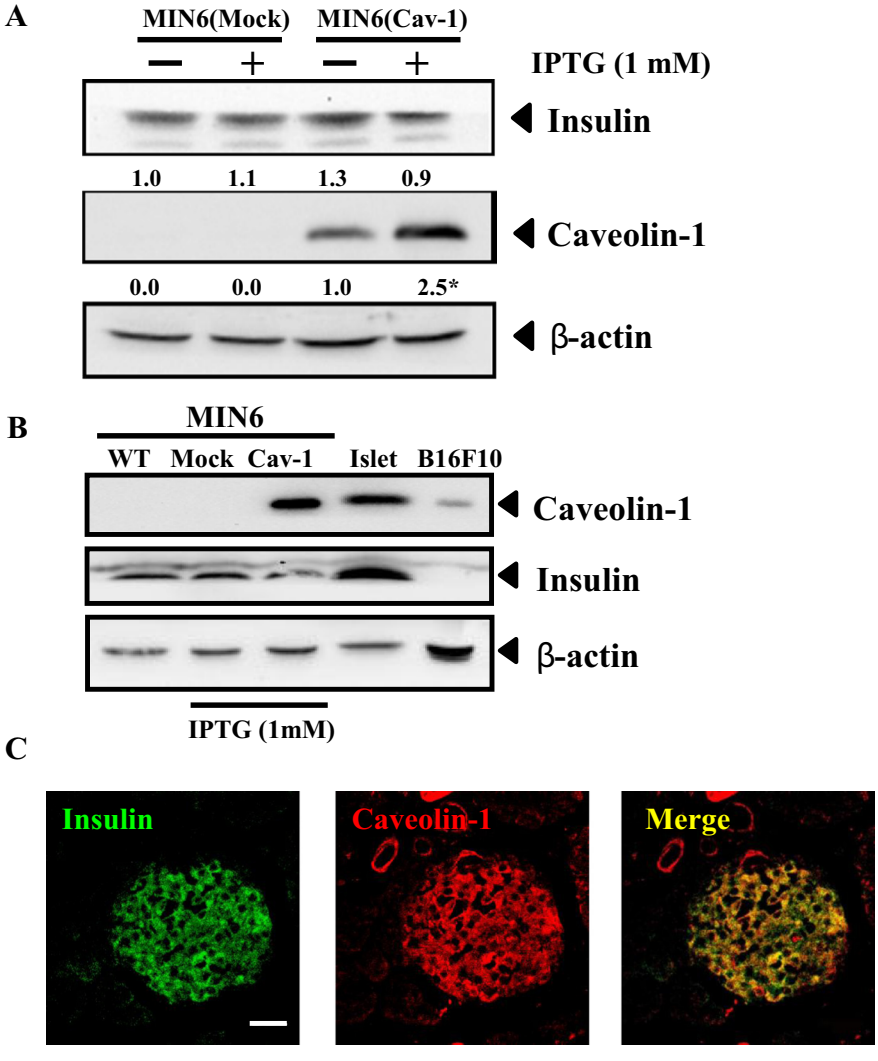

Fig. 1. Caveolin-1 expression in stably transfected MIN6 cells and isolated mouse islets. (A) MIN6 cells stably transfected with the empty vector pLacIOP (Mock) or the caveolin-1 cDNA containing pLacIOP–Cav-1 (Cav-1) vector to express caveolin-1 were incubated in DMEM high glucose with or without IPTG (1 mM) for 24 h. Then, the expression of caveolin-1, insulin and actin (control) was analyzed by western blotting. Representative blots are shown. Numerical values below the bands were obtained by scanning densitometric analysis and standardized to actin ($n = 3$; $^*p < 0.05$ comparison MIN6 (Mock) vs MIN6 (Cav-1) by Wilcoxon test). (B) Expression of caveolin-1 in wild type (WT) and stably transfected MIN6 (Mock and Cav-1) cells compared with caveolin-1 expression in isolated mouse islets. The mouse melanoma derived cell line B16F10 was used as a negative control for insulin. Note that a non-specific band migrating slightly slower than insulin was detected in all lanes. (C) Localization of caveolin-1 and insulin in mouse pancreas. A representative confocal image of a mouse pancreatic tissue section stained for caveolin-1 (red) and insulin as a marker for pancreatic β-cells (green) is shown. The merged image shown to the right (Merge) identifies caveolin-1 and insulin in a Langerhans islet. Scale bar 20 μm.

indicated in the respective figure legends. All groups analyzed were averaged from three or more independent experiments. $p < 0.05$ was considered significant.

3. Results

3.1. Characterization of stably transfected MIN6 cells

The MIN6 cells have been widely used previously as a beta pancreatic cell model of cell in various studies. Characterization of available MIN6 cells by western blotting revealed essentially undetectable levels of CAV1 (Fig. 1A). Hence, MIN6 cells were stably transfected with either the IPTG-inducible vector pLacIOP alone or encoding CAV1 (pLacIOP-cav-1), to yield MIN6 (Mock) and MIN6 (Cav-1) cells, respectively. CAV1 expression was substantially enhanced in MIN6 (Cav-1) cells (Fig. 1A). Also, we observed a significant increase in CAV1 levels when MIN6 (Cav-1) cells were incubated with IPTG for 24 h. For all subsequent experiments, 1 mM IPTG was added to the medium of MIN6 (Mock) and (Cav-1) cells. CAV1 expression was also observed in mouse (C57BL/6J) pancreatic islet extracts (Fig. 1B). In agreement with this, CAV1 was also detected in mouse pancreatic Langerhans islets by confocal microscopy where the protein colocalized to a considerable extent with insulin-containing granules (Fig. 1C).

3.2. Free fatty acids induced beta cell death

To determine whether the presence of CAV1 affects the susceptibility of MIN6 cells to free fatty acid-induced cell death, a simple flow cytometry assay was employed, based on propidium iodide cell permeability [42,43]. Indeed, palmitate, but not oleate induced, predominantly apoptotic cell death (Fig. 2A) that was more pronounced with palmitate ($^{*}p < 0.05$). Importantly, CAV1 expression in MIN6 cells enhanced palmitate-induced apoptosis in a manner that was already significant with 1 mM palmitate (Fig. 2B, $^{*}p < 0.05$). No significant changes in the necrotic sub-population were detected. To confirm that this simple cytometry assay was indeed quantifying apoptosis in MIN6 cells, several additional approaches were employed. Nuclear shrinkage and DNA fragmentation are established hallmarks of apoptosis. Thus, nuclear fragmentation was evaluated in transfected MIN6 cells exposed to free fatty acids for 24 h. As expected, palmitate (2 mM) induced nuclear fragmentation (arrows) that was more pronounced in MIN6 (Cav-1) than MIN6 (Mock) cells. In contrast, oleate treatment had no significant effect on nuclear morphology (Fig. 3A). These findings are in agreement with the flow cytometry results, given that we detected significant differences between MIN6 (Mock) and MIN6 (Cav-1) in the presence of 2 mM palmitate ($^{\#\#}p < 0.01$), with 37.5 and 51.6% of nuclear fragmentation, respectively (Fig. 3B).

In the same way, we evaluated apoptosis by quantifying caspase 3 activity using a commercially available DEVDase assay (Fig. 3C). A significant increase in caspase 3 activity ($^{***}p < 0.001$) was observed only in MIN6 (Cav-1) cells exposed to 2 mM palmitate for 24 h (Fig. 3C). This increase was statistically different from the levels presented in MIN6 (Mock) at the same palmitate concentration ($^{\#}p < 0.05$). No significant increments in caspase 3 activity were observed with 2 mM oleate ($p > 0.05$). Finally, another classic criteria employed to detect apoptosis is by observing phosphatidylserine (PS) exposure on the cell surface. Thus we additionally quantified PS accumulation using Alexa Fluor 488-conjugated annexin V. Indeed, palmitate, but not oleate,

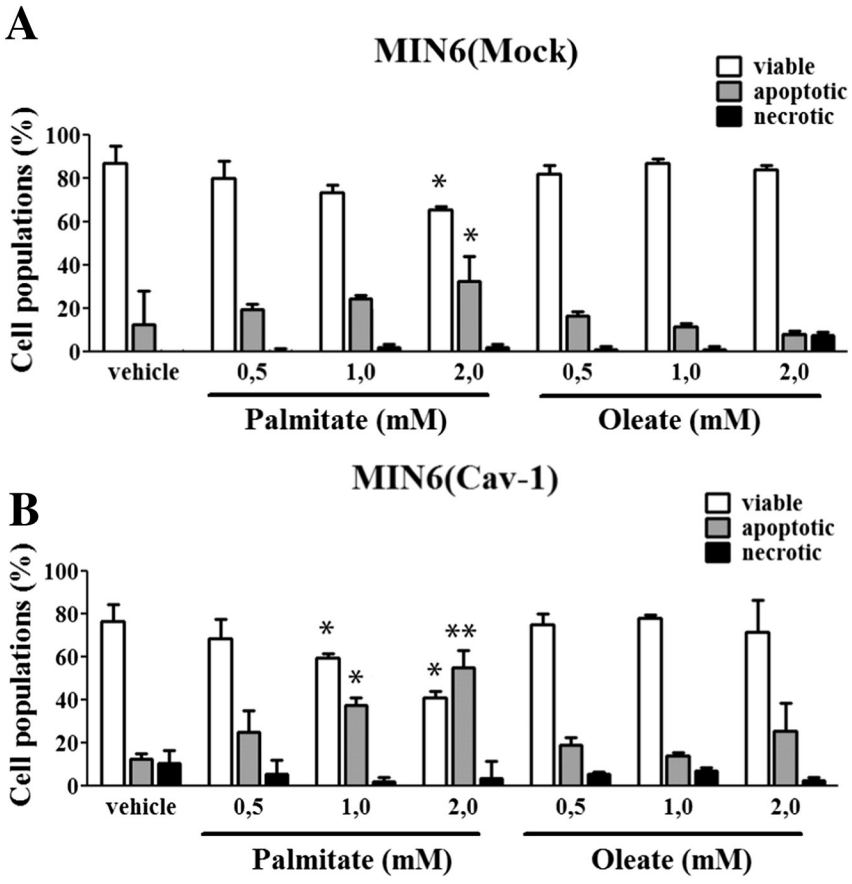

Fig. 2. Caveolin-1 expression enhanced palmitate-induced cell death. MIN6 (Mock) and MIN6 (Cav-1) were serum-starved for 12 h and then incubated with either vehicle (5.5% BSA) alone or in the presence of increasing concentrations of the free fatty acids palmitate or oleate for 24 h. Then, viability (white bars), apoptosis (gray bars) and necrosis (black bars) were determined by flow cytometric analysis following PI staining in (A) MIN6 (Mock) and (B) MIN6 (Cav-1) cells. The results shown were averaged (Mean ± SEM) from four independent experiments, and significant differences are indicated ($^{*}p < 0.05$; $^{**}p < 0.01$; with respect to vehicle, Wilcoxon test).

induced the accumulation of Annexin V-positive cells (Fig. 3D and E) in a concentration-dependent manner. Importantly, in this assay CAV1 expression in MIN6 cells enhanced palmitate-induced apoptosis (Fig. 3D, annexin V positive population) in a manner that was already significant with 0.5 mM palmitate (Fig. 2B, $^{\#}p < 0.05$). No changes in the necrotic sub-population were detected by these criteria (Fig. 3).

In summary, these results obtained using a variety of different techniques strongly suggest that palmitate, but not oleate, induced apoptosis in MIN6 cells in a manner that was potentiated by the presence of CAV1. Also, these observations validated the results obtained using the simpler PI-staining assay (see Fig. 2), by corroborating that largely palmitate-induced apoptotic cell death was being detected. This simpler assay was then employed to quantify cell death apoptosis in all subsequent experiments.

3.3. Palmitate incubation induced ceramide formation

Previous reports have shown that palmitate incubation leads to formation of ceramide, a known lipid second messenger associated with cell death [53]. For this reason, we evaluated the levels of ceramide in MIN6 (Mock) and MIN6 (Cav-1) cells exposed to palmitate, using the diacylglycerol kinase assay. Because the incubation with 2 mM palmitate induced excessive death after 24 h (>60% Fig. 2), palmitate exposure was reduced to 16 h to permit determining ceramide levels. As

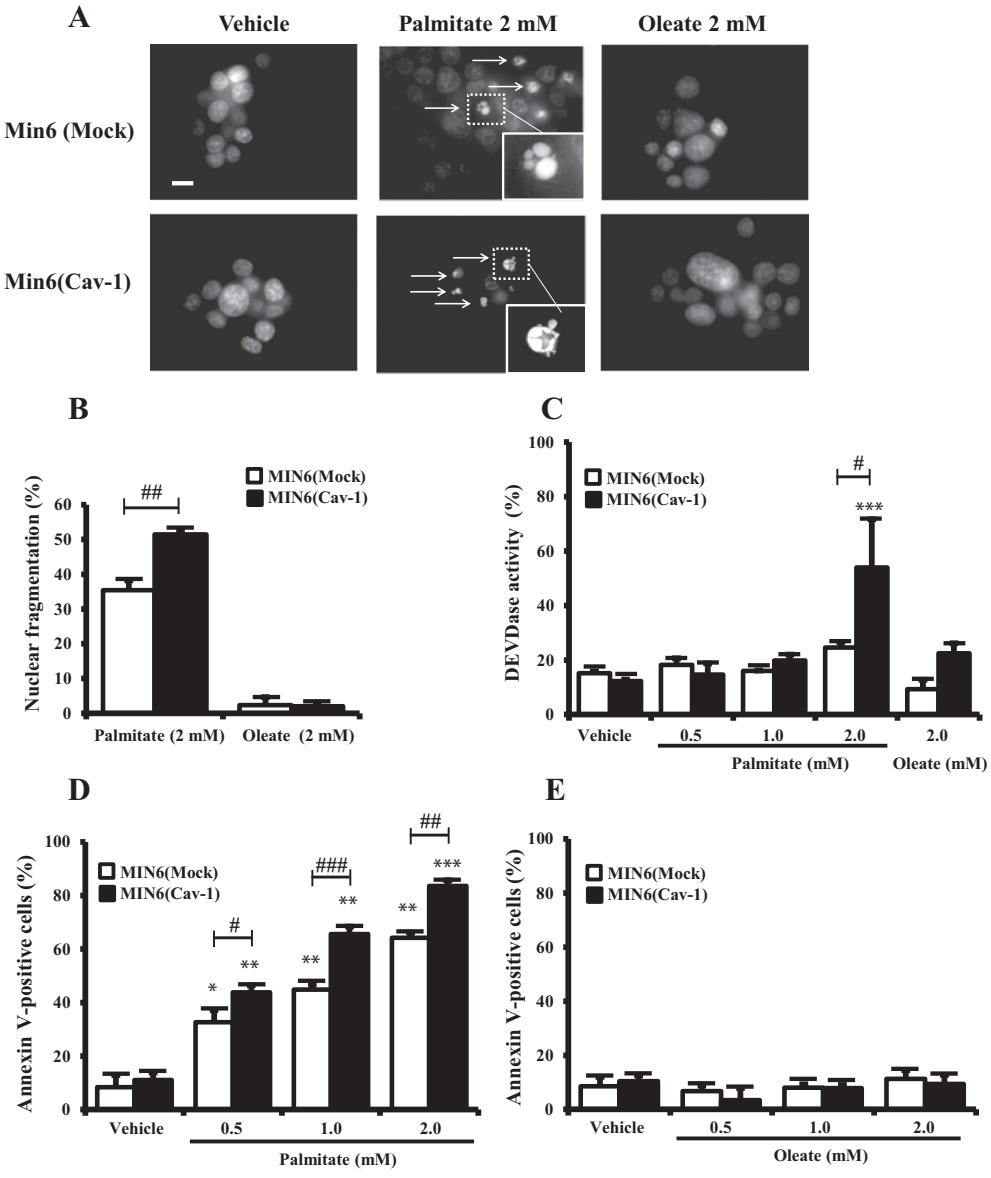

Fig. 3. Caveolin-1 expression enhanced palmitate-induced nuclear fragmentation and apoptosis. (A) MIN6 cells were grown on glass coverslips, serum deprived and then exposed to palmitate or oleate (2 mM) for 24 h, fixed, permeabilized, stained with PI and analyzed by fluorescence microscopy. Fragmented nuclei are indicated (arrows). Some fragmented nuclei (boxed) are shown at higher magnification. Magnification bar, 20 μm. (B) Hypodiploid nuclei were counted from images obtained and expressed as nuclear fragmentation (%), that is, the percentage of fragmented nuclei with respect to the total number of nuclei counted. Values shown were averaged from three independent experiments (Mean ± SEM; $^{\#\#}p < 0.01$; Mann–Whitney). The comparisons were made between MIN6 (Mock) vs MIN6 (Cav-1). (C) DEVDase activity in MIN6 (Mock) and MIN6 (Cav-1) exposed to palmitate or oleate for 24 h. Results shown were averaged (Mean ± SEM) from three independent experiments and significant differences are indicated ($^{***}p < 0.01$ with respect to vehicle, $^{\#}p < 0.05$ MIN6 (Mock) vs MIN6 (Cav-1)). (D and E) Cells were serum-starved for 12 h and then incubated with either vehicle (5.5% BSA) alone or in the presence of increasing concentrations of the free fatty acids palmitate or oleate for 24 h. Then, the cells were incubated with Alexa Fluor 488-conjugated annexin V (BD Pharmingen) and propidium iodide (Sigma) for 15 min and cellular populations were determined by flow cytometry (BD FACSCanto instrument). The percentage of total apoptotic cell populations (AV positive/PI negative and AV positive/PI positive) was determined after 24 h post-incubation with palmitate (D) and oleate (E). The results shown were averaged (Mean ± SEM) from three independent experiments and significant differences are indicated ($^{*}p < 0.05$;$^{**}p < 0.1$;$^{***}p < 0.001$ with respect to vehicle, $^{\#}p < 0.05$; $^{\#\#}p < 0.01$; $^{\#\#\#}p < 0.001$ MIN6 (Mock) vs MIN6 (Cav-1)).

shown, ceramide levels increased when MIN6 cells were incubated with palmitate (Fig. 4A), and this increase was significant in the presence of 2 mM palmitate (Fig. 4B; *$p < 0.05$). No significant differences were observed between MIN6 (Mock) and MIN6 (Cav-1), suggesting that enhanced ceramide synthesis from palmitate did not explain how CAV1 promoted palmitate induced cell-death. As expected, oleate treatment did not lead to significant changes in ceramide levels (Fig. 4B). To link palmitate-mediated effects in MIN6 cells to the de novo ceramide synthesis pathway, cells were pre-incubated with the de novo pathway inhibitors fumonisin B1 (50 μM) or myriocin (100 nM) for 30 min before adding palmitate for 16 h, and then ceramide levels were determined. Both fumonisin B1 and myriocin pre-treatment resulted in a significant decrease in ceramide levels (Fig. 4C; **$p < 0.01$). We then evaluated whether the deleterious effects induced by palmitate in MIN6 cells could be prevented by pre-incubation with de novo ceramide synthesis inhibitors (Fig. 4D). Indeed, in the presence of these inhibitors, MIN6 viability following incubation with palmitate improved, suggesting that de novo ceramide synthesis contributes to palmitate-induced cell death.

3.4. Caveolin-1 enhanced C2-ceramide and hydrogen peroxide-induced cell death in beta cells

To implicate directly ceramide synthesis following palmitate exposure, we evaluated whether CAV1 sensitized cells to ceramide-induced cell death. To this end, we incubated MIN6 (Mock) and MIN6 (Cav-1) cells with different C2-ceramide concentrations for 16 h. As shown (Fig. 5A), CAV1 expression sensitized cells to C2-ceramide-induced apoptosis at concentrations of 100 μM or higher ($^{\#}p < 0.05$). Deleterious effects of ceramide have previously been associated with ROS formation [42,54], so we evaluated whether CAV1 expression enhanced hydrogen peroxide-induced beta cell death. As shown, CAV1 presence decreased MIN6 viability compared to MIN6 (Mock) cells at or beyond 300 μM of hydrogen peroxide (Fig. 5B; $^{\#}p < 0.05$). These results suggest that

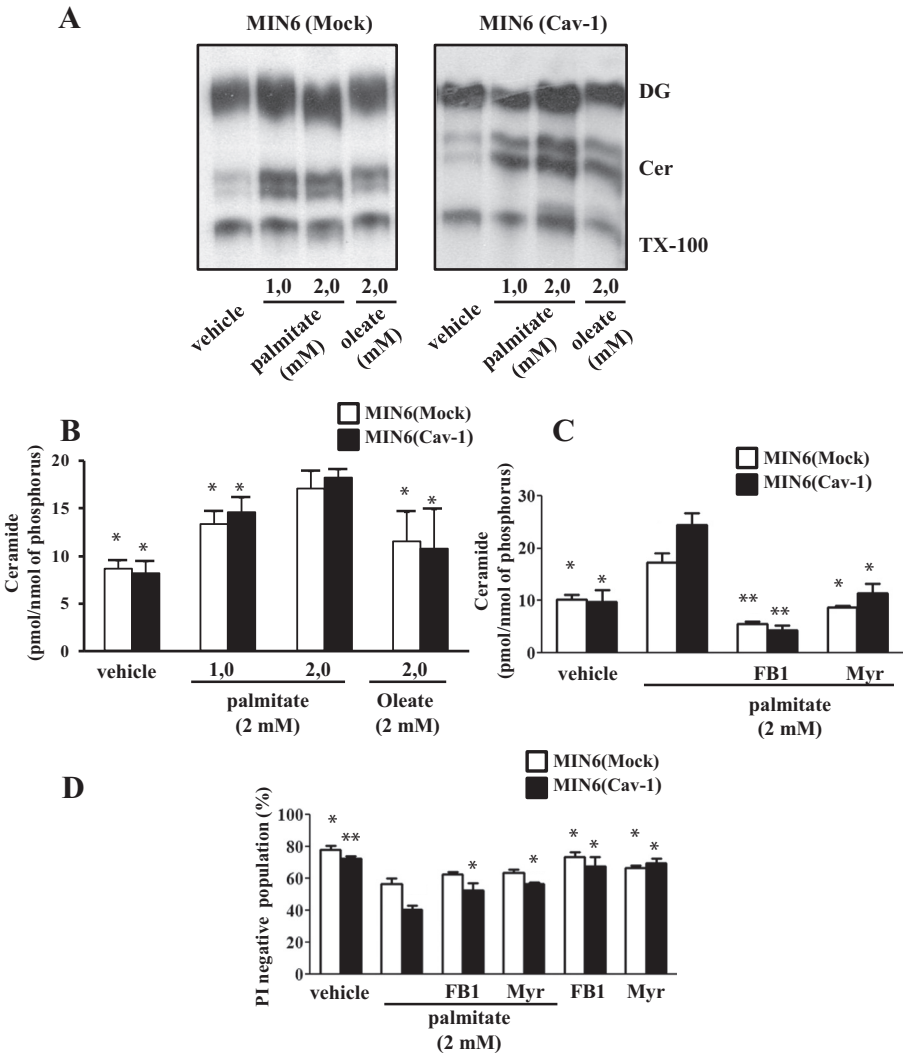

Fig. 4. Palmitate induced de novo ceramide synthesis in MIN6 cells. MIN6 (Mock) and MIN6 (Cav-1) cells were serum deprived for 12 h and then exposed to either vehicle alone or together with palmitate or oleate for 16 h. Then, lipids were extracted and ceramide levels were quantified by the diacylglycerol kinase method. Results obtained in a representative experiment after TLC are shown. (A). DG: diacylglycerol, Cer: ceramide, TX-100: Triton. (B) The bands corresponding to ceramide were scraped and quantified as described in the Materials and methods. Values shown were averaged from three independent experiments (Mean ± SEM; *$p < 0.05$, with respect to palmitate (2 mM)). MIN6 (Mock) and (Cav-1) cells were serum deprived for 12 h and then pre-incubated with inhibitors of de novo ceramide synthesis, fumonisin B1 (FB1: 50 μM) or myriocin (Myr: 100 nM) for 1 h and exposed to either vehicle alone or together with palmitate (2 mM) for another 24 h. Then, cells were either utilized for the determination of ceramide levels as described (C) or harvested and stained with PI to determine viability by flow cytometry analysis (D). Values shown were averaged from three independent experiments (Mean ± SEM; *$p < 0.05$; **$p < 0.01$; Wilcoxon test. Comparisons with respect to palmitate (2 mM) in the absence of inhibitor).

CAV1 sensitizes beta cell to death downstream of ceramide synthesis at the level of ROS production, but only when ceramide concentrations are high.

3.5. Palmitate and C2-ceramide induced ROS production in MIN6 cells was prevented by antioxidants

To assess whether CAV1 enhances ROS production, MIN6 cells were exposed to palmitate (2 mM) or C2-ceramide (200 μM) and ROS were measured by flow cytometry using DHR123 as a fluorescent probe. Palmitate and C2-ceramide both increased ROS levels (Fig. 6B and C, respectively) and in both cases the increase was significant at 4 h post-incubation. Neither the free fatty acid vehicle (BSA 5.5%) nor oleate (2 mM) induced any appreciable changes in ROS levels (Fig. 6A and D, respectively). Importantly, CAV1 expression did not produce changes in ROS generation, which suggests that the mechanism leading to CAV1 enhanced death in the presence of palmitate is located downstream of ROS generation induced by palmitate and its product, ceramide in MIN6 cells.

To evaluate the importance of ceramide generation in the ROS increment induced by palmitate, MIN6 (Mock) and MIN6 (Cav-1) cells were pre-incubated with the ceramide synthesis inhibitor myriocin (100 nM) for 1 h and then the cells were exposed to palmitate (2 mM). Addition of myriocin reduced ROS production induced by palmitate and the presence of CAV1 did not alter this observation (Fig. 7A, $^{*}p < 0.05$). To assess whether the increase in ROS generation was responsible for loss of viability upon exposure to palmitate, MIN6 cells were pre-incubated with the antioxidant: NAC (3 mM) for 1 h and then palmitate (2 mM) or C2-ceramide (200 μM) were added for 24 and 16 h, respectively. This reduction in exposure time for C2-ceramide to 16 h was necessary due to the greater toxicity to cells (Fig. 5). A significant increase in viability of cells exposed to palmitate was observed with NAC in MIN6 (Mock) and MIN6 (Cav-1) ($^{*}p < 0.05$ and $^{**}p < 0.01$) (Fig. 7B and C). These observations suggest that CAV1 enhanced death occurs downstream of ROS production likely due to localized ceramide accumulation and ROS formation as a consequence.

3.6. Palmitate and C2-ceramide exert mitochondrial damage in MIN6 cells

Because abnormal mitochondrial function is an important source of ROS [55,56], we evaluated mitochondrial membrane potential using rhodamine 123 (1 μM final concentration), which increases fluorescence upon incorporation into the membrane of functional mitochondria and decreases fluorescence if the membrane potential is lost [42,48]. We observed an increase in the percentage of MIN6 cells lacking fluorescence by roughly 50% when they were incubated with either palmitate (2 mM) or C2-ceramide (200 μM) for 4 h (Fig. 8A). Alternatively, neither oleate (2 mM) nor the biologically inactive C2-ceramide analog, C2-dihydroceramide (200 μM) leads to noticeable changes compared to the vehicle alone (5.5% BSA). In time-course assays incubation with palmitate (2 mM) up to 6 h leads to a time-dependent decrease in the percentage of fluorescence positive MIN6 (Mock) and MIN6 (Cav-1) cells, and the decrease was significant at 4 h post-incubation (Fig. 8B; $^{*}p < 0.05$). No significant differences between Min6 (Mock) and MIN6 (CAV-1) cells were observed. It should be noted that loss of mitochondrial membrane potential, correlated well with the ROS increase observed previously (Fig. 6). Thus both, palmitate and C2-ceramide induced loss of mitochondrial membrane potential (MMP), suggestive of mitochondrial damage in MIN6 cells, but in neither case did the presence of CAV1 alter loss of MMP.

3.7. Palmitate and C2-ceramide induced CAV1 phosphorylation on tyrosine-14 was blocked by the Src-family kinase inhibitor PP2

So far, our results reveal that palmitate induced ceramide synthesis, an increase in ROS generation and mitochondrial damage in MIN6 cells, but that CAV1 did not appear to alter any of these processes, although the presence of the protein did enhance apoptosis caused by palmitate. Given that oxidative stress is associated with CAV1 phosphorylation on residue tyrosine-14 by Src family kinases [30,31] and that this phenomenon has been associated with enhanced sensitivity to cell death [32,33], we evaluated whether palmitate exposure induced phosphorylation of CAV1 on tyrosine-14 (Fig. 9). MIN6 (Cav-1) cells were incubated with palmitate (2 mM) for up to 10 h and CAV1 phosphorylation on tyrosine-14 was evaluated with a specific antibody (see Materials and methods). As a positive control, cells were exposed to hydrogen peroxide (5 mM final) for 30 min. Palmitate incubation induced transient CAV1 phosphorylation, starting 2 h post-incubation, reaching a peak at 4 h and decreasing thereafter (Fig. 9A). Again, CAV1 phosphorylation correlated well with ROS generation induced by palmitate (Fig. 6). To test whether CAV1 phosphorylation was dependent on Src family kinase activity, MIN6 (Cav-1) cells were pre-incubated with the inhibitor PP2 (10 μM) for 30 min, prior to the incubation with palmitate (2 mM) or C2-ceramide (200 μM). Both palmitate- and C2-ceramide-induced CAV1 phosphorylation on tyrosine-14 were inhibited in the presence of PP2 (Fig. 9B). Taken together, these results suggest that palmitate and C2-ceramide induce CAV1 phosphorylation on tyrosine-14 in a Src-family kinase dependent manner by increasing oxidative stress in MIN6 cells.

3.8. CAV1 phosphorylation on tyrosine-14 is required to promote palmitate-induced cell death in MIN6 cells

To further examine whether Y14-phosphorylation of CAV1 by Src family kinases was necessary to promote palmitate-induced cell death, MIN6 (Mock) and MIN6 (Cav-1) cells were pre-incubated with or

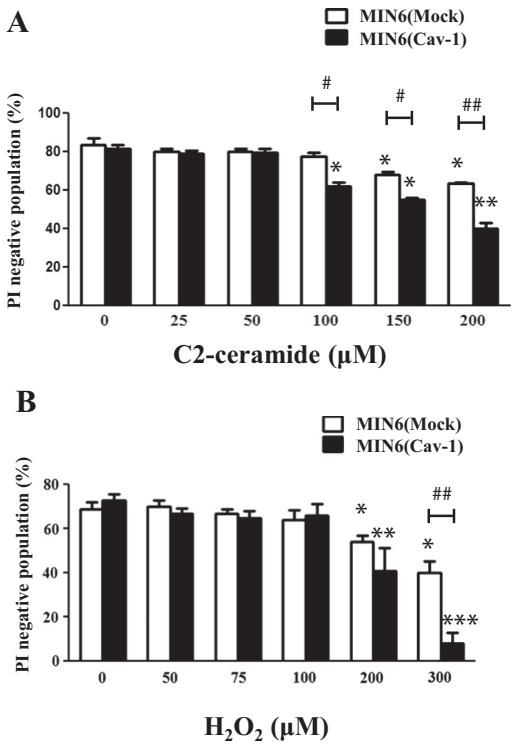

Fig. 5. Caveolin-1 expression enhanced C2-ceramide and hydrogen peroxide-induced cell death. MIN6 (Mock) and MIN6 (Cav-1) cells were serum deprived for 12 h and exposed to increasing concentrations of either C2-ceramide (A) or hydrogen peroxide (B) for 16 h. The cells were harvested, stained with PI and viability was evaluated by flow cytometry. The results shown were averaged from four independent experiments (Mean ± SEM;$^{*}p < 0.05$; $^{**}p < 0.01$; $^{***}p < 0.001$. Comparisons with respect to concentration zero; $^{\#}p < 0.05$; $^{\#\#}p < 0.01$; Wilcoxon test for intragroup comparison and Mann–Whitney for intergroup comparison).

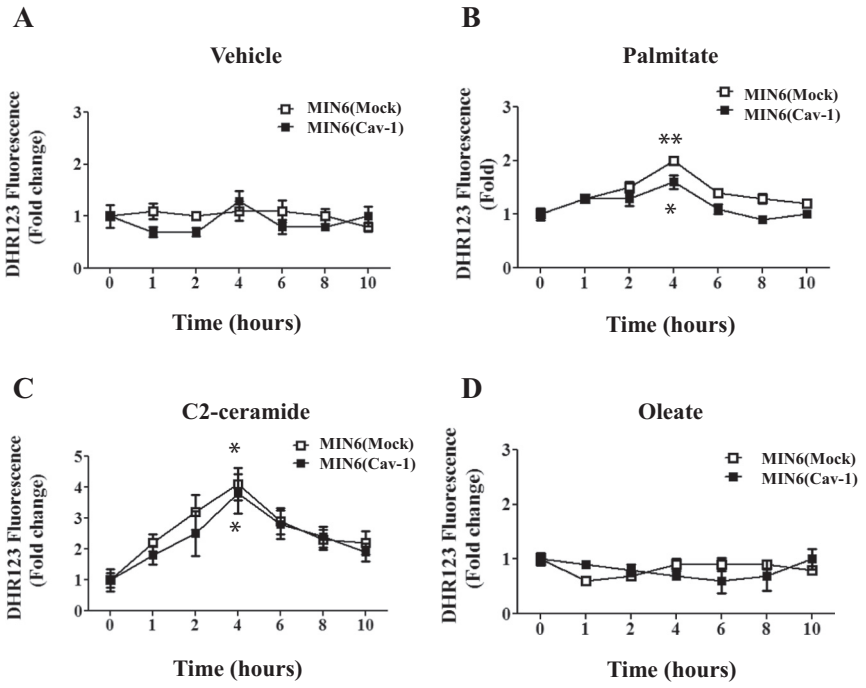

Fig. 6. Palmitate and C2-ceramide increased in ROS levels in stably transfected MIN6 cells. MIN6 (Mock) and MIN6 (Cav-1) cells were serum deprived for 12 h and then incubated with either (A) vehicle (5.5% BSA) alone or together with (B) palmitate (2 mM), (C) oleate (2 mM), or (D) C2-ceramide (200 μM) for the time points indicated up to 10 h. Subsequently, cells were labeled with dihydrorhodamine-123 (DHR123, 1 μM) for 30 min, washed, re-suspended in cold PBS and fluorescence was analyzed by flow cytometry as described. Fluorescence observed at time point zero was considered as 1. Values shown were averaged from five independent experiments (Mean ± SEM; *$p < 0.05$, **$p < 0.01$. Comparisons with respect to time point zero; 2-Way ANOVA with post-hoc multiple comparison).

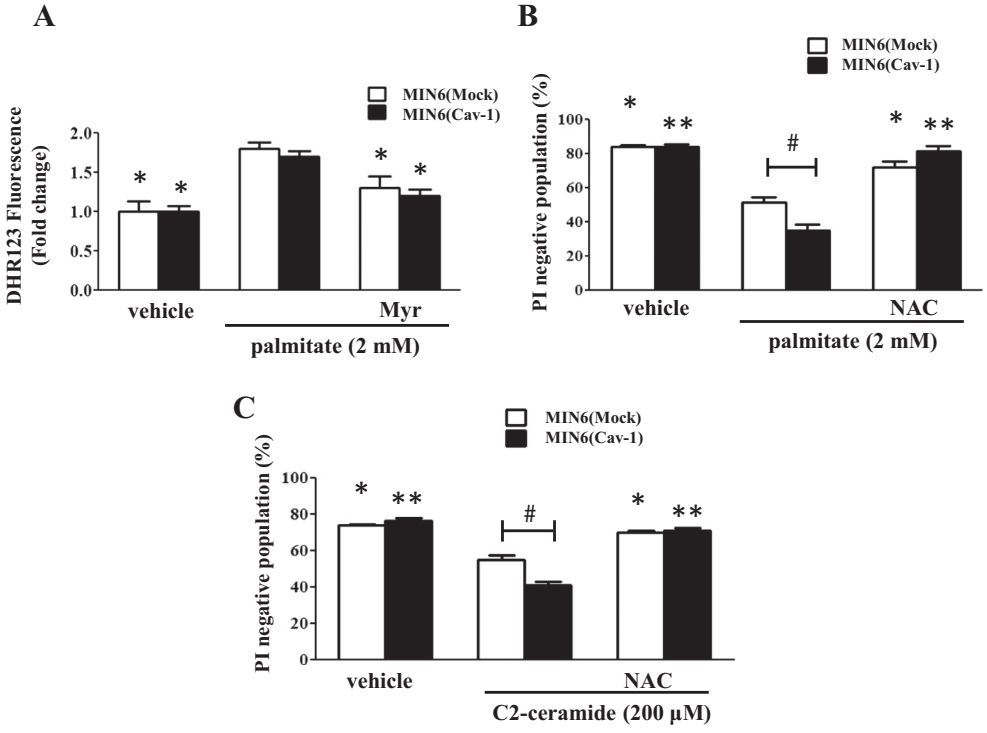

Fig. 7. Palmitate induced-ROS generation was dependent on ceramide synthesis and cytotoxicity was partially inhibited by NAC. (A) MIN6 (Mock) and MIN6 (Cav-1) cells were serum deprived for 12 h and pre-incubated with the ceramide synthesis inhibitor myriocin (Myr: 100 nM) for 1 h. Then cells were exposed to either vehicle (5.5% BSA) alone or together with palmitate (2 mM) for 16 h to determine DHR123 fluorescence (ROS formation). MIN6 (Mock) and (Cav-1) cells were pre-incubated with the anti-oxidant NAC (3 mM) for 1 h and then incubated with (B) palmitate (2 mM) for 24 h, or with (C) C2-ceramide (200 μM) for 16 h. Viability was evaluated by flow cytometry following PI staining. The values shown are averages (Mean ± SEM) from three independent experiments. Statistically significant differences in viability obtained using the Wilcoxon test for intragroup comparison and Mann–Whitney for intergroup comparison tests are indicated (*$p < 0.05$; **$p < 0.01$; with respect to palmitate (2 mM); #$p < 0.05$ (Mock) vs (Cav-1)).

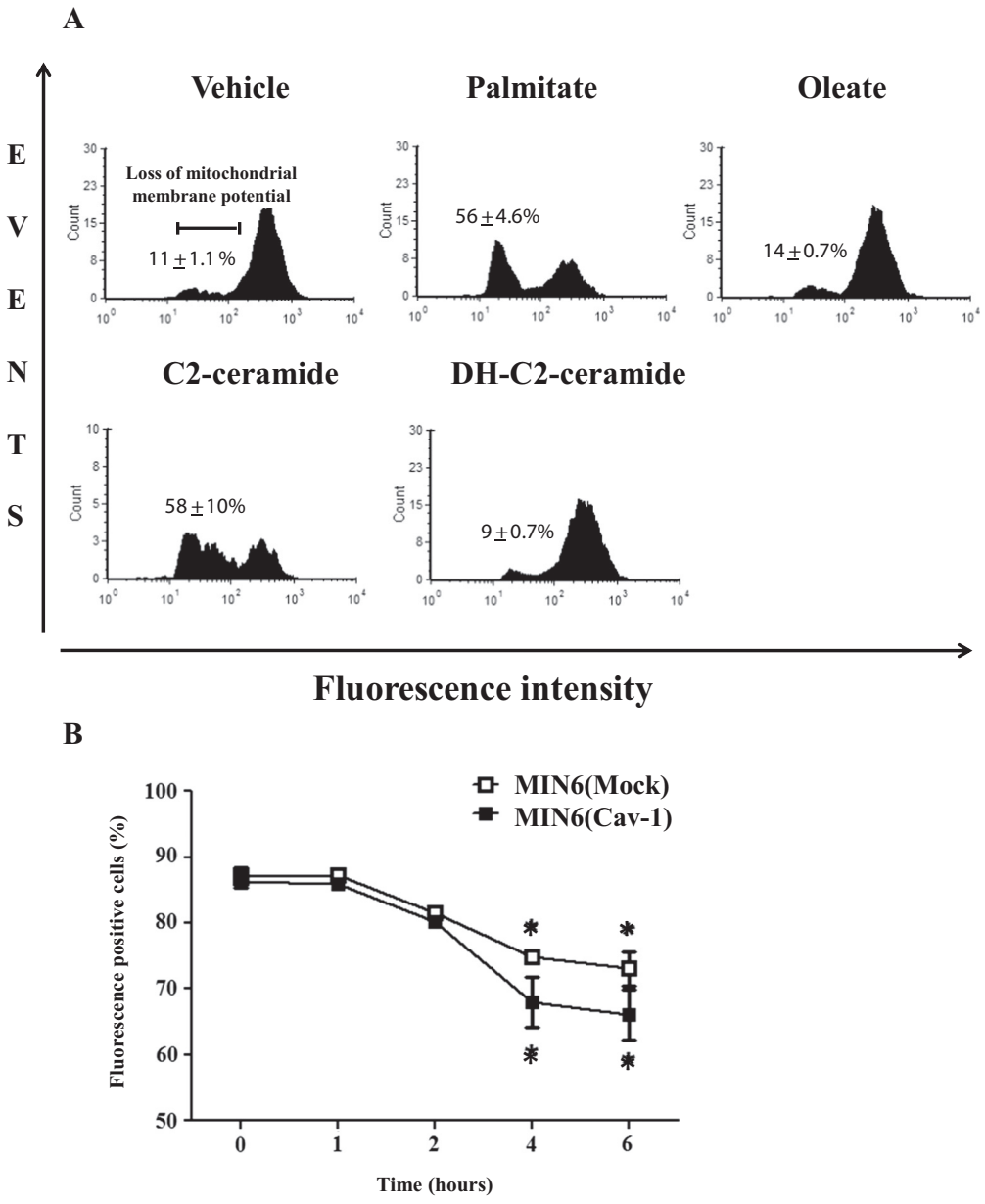

Fig. 8. Palmitate and C2-ceramide induced loss of mitochondrial membrane potential in MIN6 cells. (A) MIN6 (Mock) and MIN6 (Cav-1) cells were serum-deprived for 12 h before exposing to either vehicle (BSA 5.5%) alone or together with palmitate (2 mM), oleate (2 mM), C2-ceramide (200 μM) or DH-C2-ceramide (200 μM) for 4 h. Cells were then labeled with rhodamine 123 (1 μM final concentration) for 1 h, washed with PBS to remove the excess probe and rhodamine 123 fluorescence was analyzed by flow cytometry as described. Numerical values shown are equivalent to the percentage of fluorescence negative cells that had lost their mitochondrial membrane potential. Images show representative results for MIN6 (Cav1) cells (Mean ± SEM; n = 3). (B) MIN6 (Mock) and (Cav-1) were incubated with either vehicle (5.5% BSA) alone or together with palmitate (2 mM) for up to 6 h. After the indicated time points, cells were labeled with rhodamine 123 and fluorescence was evaluated as indicated previously. Values shown are averages (Mean ± SEM) of three independent experiments. Statistically significant differences obtained using the 2-Way ANOVA with post-hoc multiple comparison test are indicated (*$p < 0.05$ with respect to time point zero).

without PP2 (10 μM) for 1 h and then exposed to palmitate (2 mM) for 24 h (Fig. 10). An increase in the viable population was observed when MIN6 (Cav-1) cells were pre-incubated with PP2 (Fig. 10A). Importantly, this was not observed in MIN6 (Mock) cells and the differences in MIN6 (Mock) and MIN6 (Cav-1) viability in the presence of palmitate ($^{\#}p < 0.05$), disappeared with PP2. These results suggest that CAV1-enhanced cell death in the presence of palmitate was dependent on the activity of Src family kinases. In light of these results, we then evaluated the importance of CAV1 tyrosine-14 phosphorylation. To this end, MIN6 cells were stably transfected with either the phosphorylation-deficient CAV1 mutant (Y14F) or a phosphomimetic CAV1 variant (Y14E) (Fig. 10B). Then, the viability of cells expressing CAV1 wild type or the mutant proteins was evaluated in the presence of palmitate (2 mM), C2-ceramide (200 μM) or oleate (2 mM) (Fig. 10C). For MIN6 (Y14F) cells a decreased sensitivity to palmitate and C2-ceramide was observed, similar to that obtained with MIN6 (Mock) cells. On the other hand, for the cells expressing the phosphomimetic mutant version of CAV1, MIN6 (Y14E), enhanced sensitivity to palmitate and C2-ceramide, similar to that observed with MIN6 (Cav-1), was observed. As expected, oleate induced no significant changes in viability, in comparison with vehicle. Taken together, these results suggest that CAV1 phosphorylation on tyrosine-14 is required to enhance cytotoxicity of palmitate and C2-ceramide in MIN6 cells.

4. Discussion

Our results identifying palmitate as an inducer of apoptosis are in agreement with numerous previous reports. The novelty of this study

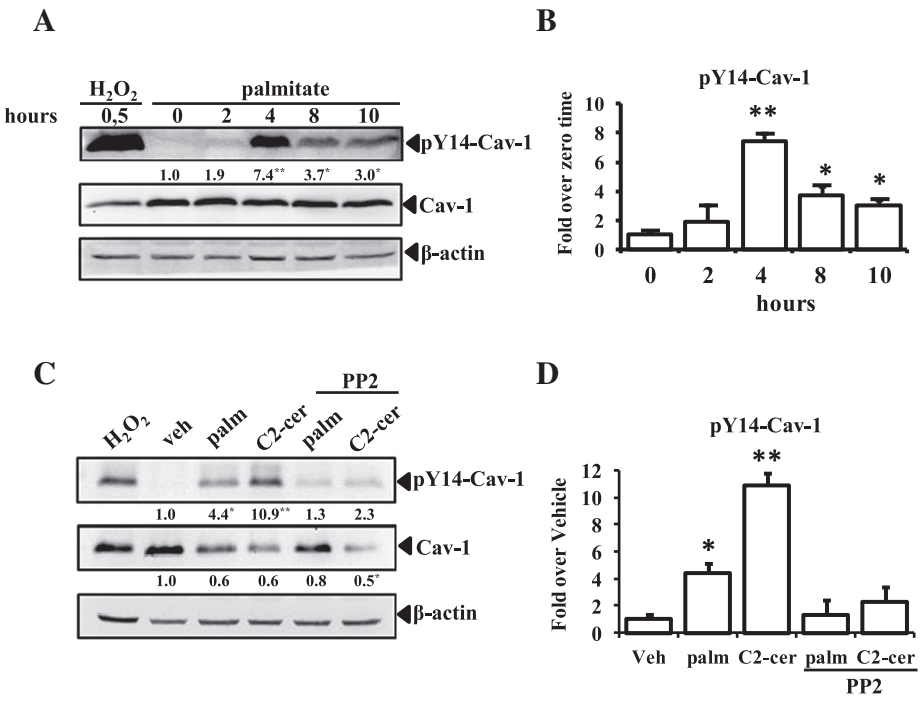

Fig. 9. Palmitate and C2-ceramide induced phosphorylation of caveolin-1 on tyrosine-14. (A) MIN6(Cav-1) cells were serum-deprived for 12 h and exposed to either vehicle (5.5% BSA) alone or together with palmitate (2 mM) for up to 10 h. Then, cell extracts were prepared and analyzed by western blotting for levels of caveolin-1, β-actin and phosphorylation of caveolin-1 on tyrosine-14. As a positive control for caveolin-1 phosphorylation, cells were incubated with H_2O_2 (5 mM final concentration) for 30 min. Blots are representative of results obtained in three independent assays. Numerical values below the bands were obtained by scanning densitometry analysis after standardizing to actin. (B) Graph depicting pY14-Cav-1 levels from (A). Values for the control without palmitate were considered as 1.0 (*$p < 0.05$, **$p < 0.01$ with respect to control; Wilcoxon test). (C) MIN6(Cav-1) cells were pre-incubated or not with the Src kinase-inhibitor PP2 (10 μM) before incubation with either H_2O_2 (positive control), vehicle alone (negative control) or together with palmitate (2 mM), oleate (2 mM) or C2-ceramide (200 μM) for 4 h. Then, the levels of caveolin-1 phosphorylated on tyrosine-14 (pY14-caveolin-1), caveolin-1 and β-actin were evaluated by western blotting. Blots are representative of results obtained in three independent assays. Numerical values below the bands were obtained by scanning densitometric analysis after standardizing to actin. (D) Graph depicting pY14-Cav-1 levels from (C). Control with only the vehicle (BSA) was considered as 1.0 (*$p < 0.05$, **$p < 0.01$ with respect to control; Wilcoxon test).

resides in showing that CAV1 expression in beta pancreatic cells renders them more sensitive to this stress situation and is followed by the identification of the mechanism involved. An important limiting factor in our study is the fact that we used only one beta cell line. Although MIN6 is a widely used and accepted in vitro model for beta cells, assays in other beta cell lines and primary beta cells are needed to confirm our results.

4.1. Levels of CAV1 in MIN6

Our results showed essentially undetectable levels of CAV1 in MIN6 cells (Fig. 1A), although this protein is normally present in pancreatic beta cells and previous reports show that MIN6 expresses detectable levels of CAV1 [38]. This discrepancy could be explained by the fact that the cells we used were acquired with a high passage (over thirty) and so they may have been subject to a selection process in which CAV1 expression was a disadvantage or simply was not required for essential cell function. Indeed, as we previously discussed, CAV1 expression is associated with cell cycle arrest and senescence [22] and in the present study, we corroborate the notion that CAV1 potentiates death responses triggered by stress conditions.

4.1. Fatty acid-induced cell death and lipid droplet formation

Over a decade ago, Shimabukuro et al. demonstrated that palmitate exposure induced apoptosis in cultured islets from Zucker diabetic fatty rats in a manner that was dependent on de novo ceramide synthesis from free fatty acids [57]. Additional studies went on to show that high levels and or prolonged exposition to free fatty acids, particularly saturated fatty acids like palmitate, induced apoptotic cell death. This phenomenon is not restricted to beta pancreatic cells, but is also observed in hepatocytes [58], vascular endothelial cells [59], skeletal muscle cells [59], cardiomyocytes [60], as well as other cell types [61,62]. In the current study, we show that palmitate exposure induced significant apoptosis in MIN6 cells after 24 h (Fig. 2), in agreement with previous studies, in which palmitate was shown to be toxic at 0.5 and 1 mM [2,7]. In our study, a tendency towards decreased viability was observed between 0.5 mM and 2.0 mM. These concentrations lie within the physiologically relevant range for free fatty acids that have been suggested to potentially mimic lipotoxicity in the context of type 2 diabetes [57]. Notably, in our experiments, oleate had no significant effect on MIN6 cell viability. Although, oleate induced-cell death has been reported, the majority of studies conclude that saturated fatty acids (like palmitate) are more cytotoxic than the unsaturated fatty acids [7,63]. Interestingly, however, some studies even suggest that oleate can protect against deleterious effects of saturated free fatty acids [13]. One possible explanation suggests that the excess oleate, in contrast to palmitate, is readily stored as triglycerides in lipid droplets in cells [64,65]. Consistent with this possibility, we observed abundant formation of lipid droplets in MIN6 cells exposed to oleate, but not with palmitate (Supplementary Fig. 1). Importantly, the toxic effects of palmitate were enhanced in MIN6 (Cav-1) cells with augmented CAV1 expression compared to MIN6 (Mock) cells (Figs. 2, 3). CAV1 expression has been previously associated with lipid droplet formation [66] and enhanced sensitivity to different cytotoxic stimuli [34–37]. Moreover, while CAV1 plays a physiologically relevant, beneficial role in insulin secretion in beta cells [38], it is also known to participate in pathological processes in these cells, including metabolic dysfunction induced by interleukin 1-beta [67]. Thus, the role of this protein in beta cells appears to be rather ambiguous. Here, for the first time, we show that CAV1 expression enhances beta

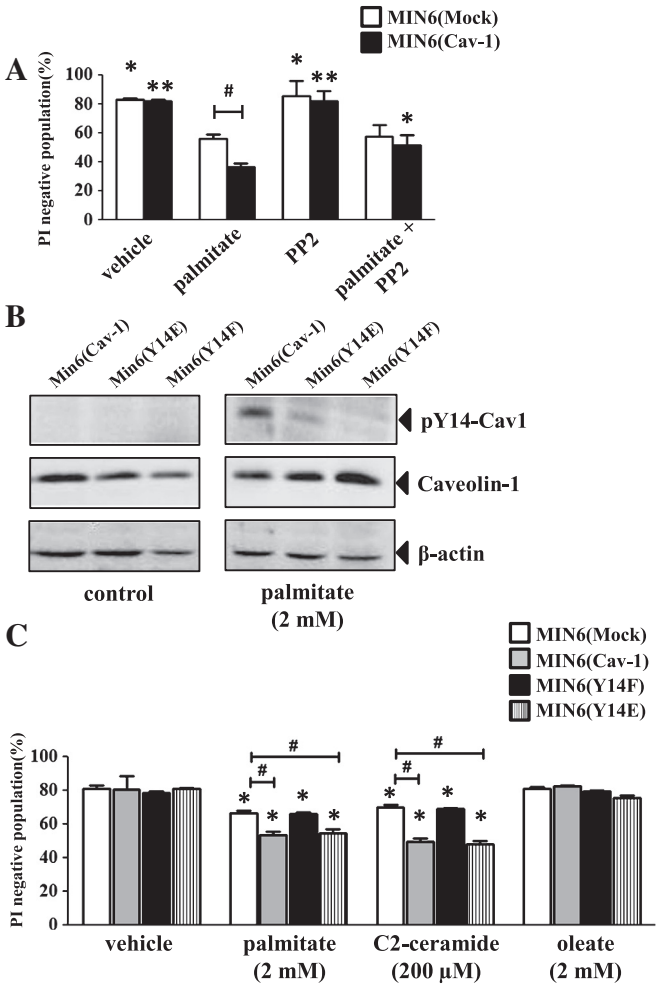

Fig. 10. Y14-phosphorylation was required for caveolin-1 to promote palmitate and C2-ceramide-induced cell death. (A) MIN6(Mock) and (Cav-1) cells were serum-deprived for 12 h, pre-incubated with or without PP2 (Src inhibitor; 10 μM) for 1 h and then incubated with either vehicle (5.5% BSA) alone or together with palmitate (2 mM) for 24 h. Then, viability was evaluated by flow cytometry following staining with PI. Data shown are averages (Mean ± SEM) obtained from three independent experiments (*$p < 0.05$; **$p < 0.01$ with respect to palmitate (2 mM); #$p < 0.05$ (Mock) vs (Cav-1)). (B) Generation of MIN6 expressing non-phosphorylatable Cav-1. MIN6 cells were stably transfected with a plasmid encoding non-phosphorylatable caveolin-1 (Y14F) or phosphomimetic caveolin-1 (Y14E). Wild type caveolin-1, caveolin-1 (Y14E) and caveolin-1 (Y14F) expressing cells, were incubated with either vehicle alone (control) or together with palmitate (palm: 2 mM) or C2-ceramide (C2-cer: 200 μM) for 4 h. Then, protein extracts were prepared and analyzed by western blotting to evaluate protein levels of β-actin, caveolin-1 and pY14-caveolin-1. The results shown are representative of three independent experiments. (C) MIN6 (Mock), MIN6(Cav-1), MIN6(Y14F) and MIN6(Y14E) cells were serum-deprived for 12 h and then incubated with either vehicle alone or together with palmitate (palm: 2 mM), oleate (ole: 2 mM) or C2-ceramide (C2-cer: 200 μM) for 24 h. Then, cells were stained with PI and the viability was analyzed by flow cytometry. Results were averaged (Mean ± SEM) from three independent experiments. Statistical differences are indicated (*$p < 0.05$ with respect to vehicle; #$p < 0.05$ (Mock) vs (Cav-1) vs (Y14F)).

pancreatic cell sensitivity to free fatty acids, particularly palmitate, although lipid droplet formation did not appear to be involved.

4.2. Palmitate-induced cell death and ceramide formation

Palmitate-associated deleterious effects and the connection to ceramide synthesis have been extensively documented in the literature. Ceramide is generated in cells by at least three different pathways: enzymatic breakdown of sphingomyelin, reacylation of sphingosine in the "salvage" pathway and de novo synthesis. In the latter case, palmitate is a precursor for ceramide synthesis [68]. Ceramide generation is often associated with cellular responses to stress situations [69]. Alternatively, ceramide reportedly modulates many cell functions, including those related to the regulation of metabolism, suggesting a possible function in obesity, diabetes and cardiovascular disease [53]. Enhanced ceramide production via the de novo pathway has been associated with cell death in hepatocytes [70] and also in beta pancreatic cells [71–75]. Importantly, we observed increased ceramide levels in MIN6 cells incubated with palmitate that were prevented by de novo ceramide synthesis inhibitors (Fig. 4C) and these inhibitors also reduced cell death following palmitate exposure (Fig. 4D). This suggests that ceramide synthesis may be responsible for palmitate-induced MIN6 cell death. However, ceramide formation was not altered by the presence of the CAV1 in MIN6, indicating that the CAV1-induced sensitization occurs via a different mechanism.

4.3. Palmitate, ceramide and ROS generation

Several studies are available linking free fatty acids to ceramide formation and oxidative stress. For instance, palmitate induces ROS liberation from the mitochondria associated with mitochondrial damage in skeletal muscle cells in a de novo ceramide synthesis-dependent manner [13]. Also, ceramide directly suppresses the respiratory chain Complex III [54] and possibly also the Complex II [76]. In our study, we obtained evidence indicating that both palmitate (2 mM) and C2-ceramide (100 μM) induced ROS formation in MIN6 (Mock) and MIN6 (Cav-1) cells (Fig. 6B and C). Increments in ROS following palmitate treatment were rapid, reaching a peak at 4 h as has been described previously [77]. In contrast, oleate did not increase ROS levels. Surprisingly, CAV1 expression seems to decrease ROS levels in MIN6 (Cav-1) in the presence of palmitate or C2-ceramide, although the observed decreases were not statistically significant ($p > 0.05$). We observed a positive correlation between de novo ceramide synthesis and ROS induction by palmitate in MIN6 cells. Indeed, ROS formation was inhibited by pre-incubation with myriocin (100 nM) (Fig. 7A). Taken together, the evidence provided suggests that the mechanism underlying CAV1-mediated sensitization to palmitate lies downstream of ROS generation in MIN6 cells.

Antioxidants have been shown to prevent free fatty acid or ceramide-induced cell death. For instance, human pancreatic islets were protected from a mixture of free fatty acids with a non-peptidyl radical scavenger [78] and similar results have been reported in rat pancreatic islets using nicotinamide as an antioxidant [79]. NAC, a glutathione precursor, has been implicated as a ROS scavenger in the protection of skeletal muscle cells against palmitate-induced damage [13]. Consistent with these observations and our working hypothesis, we observed that NAC protected MIN6 cells against palmitate-induced cell death (Fig. 7).

4.4. Loss of mitochondrial membrane potential

The mitochondria represent the main source of ROS in cells [55,56]. In beta pancreatic cells, ROS generation has been associated with gluco- and lipotoxicity that is frequently but not exclusively, attributed to alterations in the mitochondrial respiratory chain [80]. In the beta cell line INS 832/13, palmitate induces MMP loss that is prevented by fumonisin B1 [12]. In our studies, we observed that palmitate and C2-ceramide induced a significant increase ($p < 0.05$) in the fluorescence-negative MIN6 population (loss of MMP), suggesting that both agents cause mitochondrial damage in MIN6 cells (Fig. 8A). In a time-course assay, the decrease in fluorescence positive cells after 4 h coincided temporarily with the peak of ROS generation (Fig. 6), although the presence of CAV1 did not alter this tendency significantly.

Mitochondrial damage may represent both a source or the consequence of ROS formation [81]. The experiments described here were not able to distinguish between whether ROS were generated as the consequence of palmitate-induced mitochondrial damage or

alternatively, palmitate induced ROS, which in turn promoted mitochondrial damage. Ceramide has been shown to induce ROS formation by NADPH oxidase activation in endothelial cells and the same mechanism has been proposed to occur in beta cells [82] and has been associated with the development of type II diabetes mellitus [81].

On the other hand, enhanced susceptibility to oxidative stress in cells expressing CAV1 has been proposed previously. For instance, lack of CAV1 in lung fibroblasts inhibits premature senescence induced by oxidative stress triggered by cigarette smoke [83]. Along the same lines, CAV1 has been attributed a preponderant role in the "free radical theory" of aging and premature senescence [84].

4.5. CAV1 phosphorylation induced by palmitate

Our results indicate that CAV1 participates in the demise of MIN6 cells caused by palmitate and ceramide downstream of ROS production and mitochondrial damage. Thus, we evaluated the possibility that oxidative stress generated by palmitate exposure altered the "functional behavior" of CAV1 and sensitized the beta cell to apoptosis. CAV1 is known to be phosphorylated on tyrosine-14 in response to oxidative stress [29]. This phosphorylation is triggered by the activation of non-receptor tyrosine kinases including Src, Abl and Fyn due to a variety of stimuli and tyrosine-14 phosphorylation has been suggested to represent an oxidative stress marker [17,30,31,85] and sensitize to cell death [32,33]. In this study, we observed that palmitate (2 mM) induced a significant increase ($p < 0.01$) in tyrosine-14 phosphorylation, which peaked after 4 h (Fig. 9A and B) and coincided with the previously observed peak in ROS generation (Fig. 6). C2-ceramide (100 μM) also augmented CAV1 tyrosine-14 phosphorylation after 4 h (Fig. 9C and D). In both cases, tyrosine-14 phosphorylation was abolished by pre-incubation with the Src kinase inhibitor PP2 (Fig. 9C and D). Also, PP2 induced a significant increase in MIN6 (Cav-1) cell viability after exposure for 24 h to palmitate (2 mM) (Fig. 10A). Importantly, PP2 had no effects on palmitate sensitivity in MIN6 (Mock) cells, as was also the case for the ceramide synthesis inhibitors myriocin and fumonisin B1 (Fig. 4D).

These results obtained with PP2 associate palmitate exposure with the Src kinase activation through ROS generation. Src family kinases participate in a number of crucial cellular events, such as cytoskeleton remodeling, proliferation and cell signaling [29,86,87]. It has been proposed that the members of this family can be activated by ROS following oxidation of a disulfide bridge that favors maintenance of an open and completely active conformation of the enzyme [88]. In a previous study, Lyn function as redox sensor in leukocytes was attributed to oxidation of cysteine residue C466 by H_2O_2 produced during tissue injury. Cysteine oxidation leads to a conformational change and Lyn activation, which initiates pathways that regulate chemotaxis in these cells [89]. Thus, it is intriguing to suggest that palmitate exposure leads to ceramide synthesis which induces ROS formation and activates a Src family kinase member that in turn phosphorylates CAV1 on tyrosine-14.

The biological significance of CAV1 phosphorylation on tyrosine-14 is still controversial. In fact, this modification reportedly participates in caveolae formation and function [90], actin cytoskeleton remodeling and focal adhesion formation in response to oxidative stress [29]. Also, the phosphorylation of CAV1 on tyrosine-14 participates in Src inhibition through the recruitment of Csk [91]. To evaluate the relevance of tyrosine-14, we expressed in MIN6 cells a mutated version of CAV1 in which tyrosine-14 was replaced either by the non-phosphorylatable amino acid phenylalanine (Y14F) or the phosphomimetic amino acid glutamic acid (Y14E). For MIN6 (Y14F), diminished sensitivity to palmitate and C2-ceramide, similar to MIN6 (Mock) cells, was observed (Fig. 10C), while for MIN6 (Y14E) cells, sensitivity to palmitate was similar to that of MIN6 (Cav-1) cells. Taken together, these results implicate CAV1 phosphorylation on tyrosine-14 in augmented sensitivity to palmitate in MIN6 cells and specifically link enhanced sensitivity of MIN6 cells expressing CAV1 to ceramide-induced ROS formation and tyrosine-14 phosphorylation.

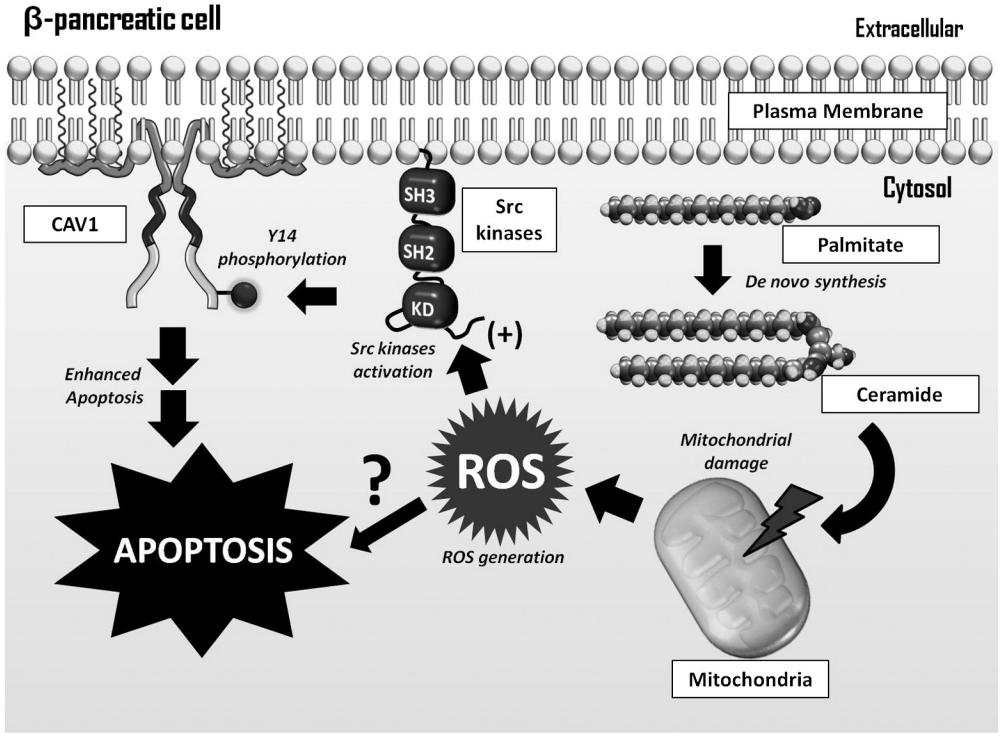

Fig. 11. Working model that summarizes the major findings described here. Palmitate is taken up by the cell and utilized as a precursor for de novo ceramide synthesis. Elevated intracellular ceramide levels, in turn, induce mitochondrial damage and increase oxidative stress. Augmented ROS levels trigger largely apoptotic beta-cell death. Additionally, ROS activate Src family kinases that phosphorylate CAV1 on tyrosine-14 and thereby enhance palmitate-induced apoptotic cell death. The model presented here provides a plausible explanation for how the expression of CAV1 sensitizes beta-cells to palmitate-induced apoptosis.

This ability of CAV1 to modulate cellular responses after tyrosine-14 phosphorylation is attributed to accessibility of the scaffolding domain of this protein. Tyrosine-14 phosphorylation is suggested to facilitate the assembly, recruitment and even the sequestration of signaling complexes, altering signaling pathways in response to a variety of stimuli [92–94]. This modification increases sensitivity to cytotoxic stress. For instance, tyrosine-14 phosphorylation of CAV1 enhances sensitivity to the chemotherapeutic agent paclitaxel in breast cancer cells, in which CAV1 serves as a scaffold protein for JNK that is activated by paclitaxel, phosphorylating BCL2 and BCLXL, which leads to inactivation of these anti-apoptotic proteins [33,92]. Phosphomimetic variants could easily replicate the effects of phosphorylation on protein conformation. However, it is difficult to envision how this change could induce appropriate docking of binding partners that recognize phosphorylated tyrosine-14. It is important to note that in our results, the phosphomimetic CAV-1 mutant Y14E showed the same response to palmitate as did wild-type CAV-1, without sensitizing cells under basal conditions (with vehicle). This is intriguing and suggests that tyrosine-14 phosphorylation need not function as a specific docking site for protein complex recruitment, but rather that changes at this site modulate CAV1 conformation in ways that are not easy to predict. Possibly the phosphomimetic modification does not replicate completely the effects on CAV1 conformation. Homology modeling of CAV1 by Shajahan et al. suggests that the aromatic ring of Tyr-14 is important due to its ability to form a stable structure that regulates protein binding to the scaffolding domain [94]. Anyway, how exactly phosphorylation of CAV1 on tyrosine-14 modulates CAV1 function remains to be defined.

With respect to the signaling downstream of phosphorylated CAV1, JNK activation is a possibility that has been linked to inflammation and beta cell dysfunction. On the other hand, the ATM-p53-p21 sequence is another interesting possibility, given that activation of this pathway has been associated with CAV1-enhanced sensitivity to oxidative stress induced-cell death in lung fibroblasts [95]. Also, CAV1 phosphorylation on Y14 is required for hyperoxia-induced apoptosis in pulmonary epithelial cells [96], where hyperoxia induces ROS production and CAV1 phosphorylation, which facilitates formation of the death-induced signaling complex (DISC) and caspase 8 activation. In our study, the signaling pathways downstream CAV1 that explain the observed pro-apoptotic effects in the presence of palmitate and ceramide, remain to be determined. Interesting possibilities include as mentioned, the MAP kinases JNK and/or p38.

5. Conclusions

In summary, we propose a working model (Fig. 11) in which palmitate enters the cell where it is employed as a precursor for de novo ceramide synthesis. The increase in intracellular ceramide levels is suggested to induce mitochondrial damage, increase ROS generation and oxidative stress in beta cells, which in turn activate pro-apoptotic pathways and cell death. Additionally, ROS activate Src family kinases that phosphorylate CAV1 on tyrosine-14, which favors the activation of pro-apoptotic pathways and in doing so, sensitizes MIN6 cells to palmitate-induced cell death. Thus, enhanced sensitivity of pancreatic beta cells to palmitate caused by the expression of CAV1 may play an important role in beta cell demise and this could be a factor to consider in the physiopathology of beta pancreatic cells. Moreover, given that CAV1 is expressed in many different cell types, it is intriguing to speculate that the presence of the protein may also sensitize those cells to palmitate-induced cell death.

Supplementary data to this article can be found online at http://dx.doi.org/10.1016/j.bbadis.2014.12.021.

Transparency document

The Transparency document associated with this article can be found, in the online version.

Acknowledgements

We thank David Mears for donating the MIN6 cells. The work presented here was supported by CONICYT Ph.D. Student Fellowships (to S. Wehinger, R. Ortiz, M. Díaz and A. Aguirre), CONICYT/FONDAP 15010006 and 15130011 (to A.F.G. Quest), FONDECYT 1090071 (to A.F.G. Quest), FONDECYT 1110149 and P-09-015F from "Iniciativas Científicas Milenio" (to L. Leyton) and ANILLO ACT1111 (to A.F.G. Quest).

References

[1] G. Patane, M. Anello, S. Piro, R. Vigneri, F. Purrello, A.M. Rabuazzo, Role of ATP production and uncoupling protein-2 in the insulin secretory defect induced by chronic exposure to high glucose or free fatty acids and effects of peroxisome proliferator-activated receptor-gamma inhibition, Diabetes 51 (2002) 2749–2756.
[2] K.H. Hellemans, J.C. Hannaert, B. Denys, K.R. Steffensen, C. Raemdonck, G.A. Martens, P.P. Van Veldhoven, J.A. Gustafsson, D. Pipeleers, Susceptibility of pancreatic beta cells to fatty acids is regulated by LXR/PPARalpha-dependent stearoyl-coenzyme A desaturase, PLoS One 4 (2009) e7266.
[3] V. Poitout, R.P. Robertson, Glucolipotoxicity: fuel excess and beta-cell dysfunction, Endocr. Rev. 29 (2008) 351–366.
[4] J.W. Kim, K.H. Yoon, Glucolipotoxicity in pancreatic beta-cells, Diabetes Metab. J. 35 (2011) 444–450.
[5] Y. Lee, H. Hirose, M. Ohneda, J.H. Johnson, J.D. McGarry, R.H. Unger, Beta-cell lipotoxicity in the pathogenesis of non-insulin-dependent diabetes mellitus of obese rats: impairment in adipocyte–beta-cell relationships, Proc. Natl. Acad. Sci. U. S. A. 91 (1994) 10878–10882.
[6] K. Sawada, K. Kawabata, T. Yamashita, K. Kawasaki, N. Yamamoto, H. Ashida, Ameliorative effects of polyunsaturated fatty acids against palmitic acid-induced insulin resistance in L6 skeletal muscle cells, Lipids Health Dis. 11 (2012) 36.
[7] E. Karaskov, C. Scott, L. Zhang, T. Teodoro, M. Ravazzola, A. Volchuk, Chronic palmitate but not oleate exposure induces endoplasmic reticulum stress, which may contribute to INS-1 pancreatic beta-cell apoptosis, Endocrinology 147 (2006) 3398–3407.
[8] W. Gehrmann, M. Elsner, S. Lenzen, Role of metabolically generated reactive oxygen species for lipotoxicity in pancreatic beta-cells, Diabetes Obes. Metab. 12 (Suppl. 2) (2010) 149–158.
[9] M. Elsner, W. Gehrmann, S. Lenzen, Peroxisome-generated hydrogen peroxide as important mediator of lipotoxicity in insulin-producing cells, Diabetes 60 (2011) 200–208.
[10] N. Lin, H. Chen, H. Zhang, X. Wan, Q. Su, Mitochondrial reactive oxygen species (ROS) inhibition ameliorates palmitate-induced INS-1 beta cell death, Endocrine 42 (2012) 107–117.
[11] R.G. Mirmira, Saturated free fatty acids: islet beta cell "stressERs", Endocrine 42 (2012) 1–2.
[12] I. Syed, B. Jayaram, W. Subasinghe, A. Kowluru, Tiam1/Rac1 signaling pathway mediates palmitate-induced, ceramide-sensitive generation of superoxides and lipid peroxides and the loss of mitochondrial membrane potential in pancreatic beta-cells, Biochem. Pharmacol. 80 (2010) 874–883.
[13] L. Yuzefovych, G. Wilson, L. Rachek, Different effects of oleate vs. palmitate on mitochondrial function, apoptosis, and insulin signaling in L6 skeletal muscle cells: role of oxidative stress, Am. J. Physiol. Endocrinol. Metab. 299 (2010) E1096–E1105.
[14] Z. Tang, P.E. Scherer, T. Okamoto, K. Song, C. Chu, D.S. Kohtz, I. Nishimoto, H.F. Lodish, M.P. Lisanti, Molecular cloning of caveolin-3, a novel member of the caveolin gene family expressed predominantly in muscle, J. Biol. Chem. 271 (1996) 2255–2261.
[15] P.E. Scherer, Z. Tang, M. Chun, M. Sargiacomo, H.F. Lodish, M.P. Lisanti, Caveolin isoforms differ in their N-terminal protein sequence and subcellular distribution. Identification and epitope mapping of an isoform-specific monoclonal antibody probe, J. Biol. Chem. 270 (1995) 16395–16401.
[16] H. Cao, W.E. Courchesne, C.C. Mastick, A phosphotyrosine-dependent protein interaction screen reveals a role for phosphorylation of caveolin-1 on tyrosine 14: recruitment of C-terminal Src kinase, J. Biol. Chem. 277 (2002) 8771–8774.
[17] S. Li, R. Seitz, M.P. Lisanti, Phosphorylation of caveolin by src tyrosine kinases. The alpha-isoform of caveolin is selectively phosphorylated by v-Src in vivo, J. Biol. Chem. 271 (1996) 3863–3868.
[18] A.F. Quest, L. Leyton, M. Parraga, Caveolins, caveolae, and lipid rafts in cellular transport, signaling, and disease, Biochem. Cell Biol. 82 (2004) 129–144.
[19] F. Bender, M. Montoya, V. Monardes, L. Leyton, A.F. Quest, Caveolae and caveolae-like membrane domains in cellular signaling and disease: identification of downstream targets for the tumor suppressor protein caveolin-1, Biol. Res. 35 (2002) 151–167.
[20] P. Liu, M. Rudick, R.G. Anderson, Multiple functions of caveolin-1, J. Biol. Chem. 277 (2002) 41295–41298.
[21] F. Galbiati, D. Volonte, J. Liu, F. Capozza, P.G. Frank, L. Zhu, R.G. Pestell, M.P. Lisanti, Caveolin-1 expression negatively regulates cell cycle progression by inducing G(0)/G(1) arrest via a p53/p21(WAF1/Cip1)-dependent mechanism, Mol. Biol. Cell 12 (2001) 2229–2244.
[22] D. Volonte, K. Zhang, M.P. Lisanti, F. Galbiati, Expression of caveolin-1 induces premature cellular senescence in primary cultures of murine fibroblasts, Mol. Biol. Cell 13 (2002) 2502–2517.

[23] A.F. Quest, J.L. Gutierrez-Pajares, V.A. Torres, Caveolin-1: an ambiguous partner in cell signalling and cancer, J. Cell. Mol. Med. 12 (2008) 1130–1150.
[24] A.F. Quest, L. Lobos-Gonzalez, S. Nunez, C. Sanhueza, J.G. Fernandez, A. Aguirre, D. Rodriguez, L. Leyton, V. Torres, The caveolin-1 connection to cell death and survival, Curr. Mol. Med. 13 (2013) 266–281.
[25] J.A. Engelman, C.C. Wykoff, S. Yasuhara, K.S. Song, T. Okamoto, M.P. Lisanti, Recombinant expression of caveolin-1 in oncogenically transformed cells abrogates anchorage-independent growth, J. Biol. Chem. 272 (1997) 16374–16381.
[26] J. Liu, P. Lee, F. Galbiati, R.N. Kitsis, M.P. Lisanti, Caveolin-1 expression sensitizes fibroblastic and epithelial cells to apoptotic stimulation, Am. J. Physiol. Cell Physiol. 280 (2001) C823–C835.
[27] V.A. Torres, J.C. Tapia, D.A. Rodriguez, M. Parraga, P. Lisboa, M. Montoya, L. Leyton, A.F. Quest, Caveolin-1 controls cell proliferation and cell death by suppressing expression of the inhibitor of apoptosis protein survivin, J. Cell Sci. 119 (2006) 1812–1823.
[28] S. Li, J. Couet, M.P. Lisanti, Src tyrosine kinases, Galpha subunits, and H-Ras share a common membrane-anchored scaffolding protein, caveolin. Caveolin binding negatively regulates the auto-activation of Src tyrosine kinases, J. Biol. Chem. 271 (1996) 29182–29190.
[29] A.R. Sanguinetti, C.C. Mastick, c-Abl is required for oxidative stress-induced phosphorylation of caveolin-1 on tyrosine 14, Cell. Signal. 15 (2003) 289–298.
[30] D. Volonte, F. Galbiati, R.G. Pestell, M.P. Lisanti, Cellular stress induces the tyrosine phosphorylation of caveolin-1 (Tyr(14)) via activation of p38 mitogen-activated protein kinase and c-Src kinase. Evidence for caveolae, the actin cytoskeleton, and focal adhesions as mechanical sensors of osmotic stress, J. Biol. Chem. 276 (2001) 8094–8103.
[31] D.B. Chen, S.M. Li, X.X. Qian, C. Moon, J. Zheng, Tyrosine phosphorylation of caveolin 1 by oxidative stress is reversible and dependent on the c-src tyrosine kinase but not mitogen-activated protein kinase pathways in placental artery endothelial cells, Biol. Reprod. 73 (2005) 761–772.
[32] H. Kim, C. Moon, M. Ahn, Y. Matsumoto, C.S. Koh, M.D. Kim, T. Shin, Increased phosphorylation of caveolin-1 in the sciatic nerves of Lewis rats with experimental autoimmune neuritis, Brain Res. 1137 (2007) 153–160.
[33] A.N. Shajahan, A. Wang, M. Decker, R.D. Minshall, M.C. Liu, R. Clarke, Caveolin-1 tyrosine phosphorylation enhances paclitaxel-mediated cytotoxicity, J. Biol. Chem. 282 (2007) 5934–5943.
[34] P. Palozza, R. Sestito, N. Picci, P. Lanza, G. Monego, F.O. Ranelletti, The sensitivity to beta-carotene growth-inhibitory and proapoptotic effects is regulated by caveolin-1 expression in human colon and prostate cancer cells, Carcinogenesis 29 (2008) 2153–2161.
[35] S. Shack, X.T. Wang, G.C. Kokkonen, M. Gorospe, D.L. Longo, N.J. Holbrook, Caveolin-induced activation of the phosphatidylinositol 3-kinase/Akt pathway increases arsenite cytotoxicity, Mol. Cell. Biol. 23 (2003) 2407–2414.
[36] H.L. Yang, W.Q. Chen, X. Cao, A. Worschech, L.F. Du, W.Y. Fang, Y.Y. Xu, D.F. Stroncek, X. Li, E. Wang, F.M. Marincola, Caveolin-1 enhances resveratrol-mediated cytotoxicity and transport in a hepatocellular carcinoma model, J. Transl. Med. 7 (2009) 22.
[37] Y.N. Jiang, Y.H. Li, M.W. Ke, T.Y. Tseng, Y.B. Tang, M.C. Huang, W.T. Cheng, Y.T. Ju, Caveolin-1 sensitizes rat pituitary adenoma GH3 cells to bromocriptine induced apoptosis, Cancer Cell Int. 7 (2007) 1.
[38] A.K. Nevins, D.C. Thurmond, Caveolin-1 functions as a novel Cdc42 guanine nucleotide dissociation inhibitor in pancreatic beta-cells, J. Biol. Chem. 281 (2006) 18961–18972.
[39] E.M. Kepner, S.M. Yoder, E. Oh, M.A. Kalwat, Z. Wang, L.A. Quilliam, D.C. Thurmond, Cool-1/betaPIX functions as a guanine nucleotide exchange factor in the cycling of Cdc42 to regulate insulin secretion, Am. J. Physiol. Endocrinol. Metab. 301 (2011) E1072–E1080.
[40] F.C. Bender, M.A. Reymond, C. Bron, A.F. Quest, Caveolin-1 levels are down-regulated in human colon tumors, and ectopic expression of caveolin-1 in colon carcinoma cell lines reduces cell tumorigenicity, Cancer Res. 60 (2000) 5870–5878.
[41] A. Duttaroy, C.L. Zimliki, D. Gautam, Y. Cui, D. Mears, J. Wess, Muscarinic stimulation of pancreatic insulin and glucagon release is abolished in m3 muscarinic acetylcholine receptor-deficient mice, Diabetes 53 (2004) 1714–1720.
[42] J. Villena, M. Henriquez, V. Torres, F. Moraga, J. Diaz-Elizondo, C. Arredondo, M. Chiong, C. Olea-Azar, A. Stutzin, S. Lavandero, A.F. Quest, Ceramide-induced formation of ROS and ATP depletion trigger necrosis in lymphoid cells, Free Radic. Biol. Med. 44 (2008) 1146–1160.
[43] C.A. Hetz, M. Hunn, P. Rojas, V. Torres, L. Leyton, A.F. Quest, Caspase-dependent initiation of apoptosis and necrosis by the Fas receptor in lymphoid cells: onset of necrosis is associated with delayed ceramide increase, J. Cell Sci. 115 (2002) 4671–4683.
[44] M. Valenzuela, C. Glorieux, J. Stockis, B. Sid, J.M. Sandoval, K.B. Felipe, M.R. Kviecinski, J. Verrax, P. Buc Calderon, Retinoic acid synergizes ATO-mediated cytotoxicity by precluding Nrf2 activity in AML cells, Br. J. Cancer 111 (2014) 874–882.
[45] E.G. Bligh, W.J. Dyer, A rapid method of total lipid extraction and purification, Can. J. Biochem. Physiol. 37 (1959) 911–917.
[46] J.P. Walsh, R.M. Bell, sn-1,2-Diacylglycerol kinase of *Escherichia coli*. Mixed micellar analysis of the phospholipid cofactor requirement and divalent cation dependence, J. Biol. Chem. 261 (1986) 6239–6247.
[47] B.N. Ames, D.T. Dubin, The role of polyamines in the neutralization of bacteriophage deoxyribonucleic acid, J. Biol. Chem. 235 (1960) 769–775.
[48] R.K. Emaus, R. Grunwald, J.J. Lemasters, Rhodamine 123 as a probe of transmembrane potential in isolated rat-liver mitochondria: spectral and metabolic properties, Biochim. Biophys. Acta 850 (1986) 436–448.
[49] H.A. Jensen, L.E. Styskal, R. Tasseff, R.P. Bunaciu, J. Congleton, J.D. Varner, A. Yen, The Src-family kinase inhibitor PP2 rescues inducible differentiation events in emergent retinoic acid-resistant myeloblastic leukemia cells, PLoS One 8 (2013) e58621.
[50] L. Kong, Z. Deng, H. Shen, Y. Zhang, Src family kinase inhibitor PP2 efficiently inhibits cervical cancer cell proliferation through down-regulating phospho-Src-Y416 and phospho-EGFR-Y1173, Mol. Cell. Biochem. 348 (2011) 11–19.
[51] Y. Wang, Y. Zhan, R. Xu, R. Shao, J. Jiang, Z. Wang, Src mediates extracellular signal-regulated kinase 1/2 activation and autophagic cell death induced by cardiac glycosides in human non-small cell lung cancer cell lines, Mol. Carcinog. (2014). http://dx.doi.org/10.1002/mc.22147.
[52] L. Janderova, M. McNeil, A.N. Murrell, R.L. Mynatt, S.R. Smith, Human mesenchymal stem cells as an in vitro model for human adipogenesis, Obes. Res. 11 (2003) 65–74.
[53] B.T. Bikman, S.A. Summers, Ceramides as modulators of cellular and whole-body metabolism, J. Clin. Invest. 121 (2011) 4222–4230.
[54] C. Garcia-Ruiz, A. Colell, M. Mari, A. Morales, J.C. Fernandez-Checa, Direct effect of ceramide on the mitochondrial electron transport chain leads to generation of reactive oxygen species. Role of mitochondrial glutathione, J. Biol. Chem. 272 (1997) 11369–11377.
[55] G. Lenaz, The mitochondrial production of reactive oxygen species: mechanisms and implications in human pathology, IUBMB Life 52 (2001) 159–164.
[56] J.F. Turrens, Mitochondrial formation of reactive oxygen species, J. Physiol. 552 (2003) 335–344.
[57] M. Shimabukuro, M. Higa, Y.T. Zhou, M.Y. Wang, C.B. Newgard, R.H. Unger, Lipoapoptosis in beta-cells of obese prediabetic fa/fa rats. Role of serine palmitoyltransferase overexpression, J. Biol. Chem. 273 (1998) 32487–32490.
[58] X. Dou, Z. Wang, T. Yao, Z. Song, Cysteine aggravates palmitate-induced cell death in hepatocytes, Life Sci. 89 (2011) 878–885.
[59] L.I. Rachek, S.I. Musiyenko, S.P. LeDoux, G.L. Wilson, Palmitate induced mitochondrial deoxyribonucleic acid damage and apoptosis in l6 rat skeletal muscle cells, Endocrinology 148 (2007) 293–299.
[60] G.C. Sparagna, D.L. Hickson-Bick, L.M. Buja, J.B. McMillin, Fatty acid-induced apoptosis in neonatal cardiomyocytes: redox signaling, Antioxid. Redox Signal. 3 (2001) 71–79.
[61] S. Hardy, W. El-Assaad, E. Przybytkowski, E. Joly, M. Prentki, Y. Langelier, Saturated fatty acid-induced apoptosis in MDA-MB-231 breast cancer cells. A role for cardiolipin, J. Biol. Chem. 278 (2003) 31861–31870.
[62] J.M. Cacicedo, S. Benjachareowong, E. Chou, N.B. Ruderman, Y. Ido, Palmitate-induced apoptosis in cultured bovine retinal pericytes: roles of NAD(P)H oxidase, oxidant stress, and ceramide, Diabetes 54 (2005) 1838–1845.
[63] D.A. Cunha, P. Hekerman, L. Ladriere, A. Bazarra-Castro, F. Ortis, M.C. Wakeham, F. Moore, J. Rasschaert, A.K. Cardozo, E. Bellomo, L. Overbergh, C. Mathieu, R. Lupi, T. Hai, A. Herchuelz, P. Marchetti, G.A. Rutter, D.L. Eizirik, M. Cnop, Initiation and execution of lipotoxic ER stress in pancreatic beta-cells, J. Cell Sci. 121 (2008) 2308–2318.
[64] M. Cnop, J.C. Hannaert, A. Hoorens, D.L. Eizirik, D.G. Pipeleers, Inverse relationship between cytotoxicity of free fatty acids in pancreatic islet cells and cellular triglyceride accumulation, Diabetes 50 (2001) 1771–1777.
[65] L.L. Listenberger, X. Han, S.E. Lewis, S. Cases, R.V. Farese Jr., D.S. Ory, J.E. Schaffer, Triglyceride accumulation protects against fatty acid-induced lipotoxicity, Proc. Natl. Acad. Sci. U. S. A. 100 (2003) 3077–3082.
[66] C.M. Blouin, S. Le Lay, A. Eberl, H.C. Kofeler, I.C. Guerrera, C. Klein, X. Le Liepvre, F. Lasnier, O. Bourron, J.F. Gautier, P. Ferre, E. Hajduch, I. Dugail, Lipid droplet analysis in caveolin-deficient adipocytes: alterations in surface phospholipid composition and maturation defects, J. Lipid Res. 51 (2010) 945–956.
[67] R. Veluthakal, I. Chvyrkova, M. Tannous, P. McDonald, R. Amin, T. Hadden, D.C. Thurmond, M.J. Quon, A. Kowluru, Essential role for membrane lipid rafts in interleukin-1beta-induced nitric oxide release from insulin-secreting cells: potential regulation by caveolin-1+, Diabetes 54 (2005) 2576–2585.
[68] A.H. Merrill Jr., De novo sphingolipid biosynthesis: a necessary, but dangerous, pathway, J. Biol. Chem. 277 (2002) 25843–25846.
[69] Y.A. Hannun, Functions of ceramide in coordinating cellular responses to stress, Science 274 (1996) 1855–1859.
[70] D. Gao, S. Nong, X. Huang, Y. Lu, H. Zhao, Y. Lin, Y. Man, S. Wang, J. Yang, J. Li, The effects of palmitate on hepatic insulin resistance are mediated by NADPH Oxidase 3-derived reactive oxygen species through JNK and p38MAPK pathways, J. Biol. Chem. 285 (2010) 29965–29973.
[71] J. Veret, N. Coant, E.V. Berdyshev, A. Skobeleva, N. Therville, D. Bailbe, I. Gorshkova, V. Natarajan, B. Portha, H. Le Stunff, Ceramide synthase 4 and de novo production of ceramides with specific N-acyl chain lengths are involved in glucolipotoxicity-induced apoptosis of INS-1 beta-cells, Biochem. J. 438 (2011) 177–189.
[72] R. Lupi, F. Dotta, L. Marselli, S. Del Guerra, M. Masini, C. Santangelo, G. Patane, U. Boggi, S. Piro, M. Anello, E. Bergamini, F. Mosca, U. Di Mario, S. Del Prato, P. Marchetti, Prolonged exposure to free fatty acids has cytostatic and pro-apoptotic effects on human pancreatic islets: evidence that beta-cell death is caspase mediated, partially dependent on ceramide pathway, and Bcl-2 regulated, Diabetes 51 (2002) 1437–1442.
[73] M. Shimabukuro, Y.T. Zhou, M. Levi, R.H. Unger, Fatty acid-induced beta cell apoptosis: a link between obesity and diabetes, Proc. Natl. Acad. Sci. U. S. A. 95 (1998) 2498–2502.
[74] F. Assimacopoulos-Jeannet, Fat storage in pancreas and in insulin-sensitive tissues in pathogenesis of type 2 diabetes, Int. J. Obes. Relat. Metab. Disord. 28 (Suppl. 4) (2004) S53–S57.
[75] K. Maedler, G.A. Spinas, D. Dyntar, W. Moritz, N. Kaiser, M.Y. Donath, Distinct effects of saturated and monounsaturated fatty acids on beta-cell turnover and function, Diabetes 50 (2001) 69–76.
[76] S.A. Novgorodov, T.I. Gudz, Ceramide and mitochondria in ischemic brain injury, Int. J. Biochem. Mol. Biol. 2 (2011) 347–361.
[77] J.Y. Park, M.J. Kim, Y.K. Kim, J.S. Woo, Ceramide induces apoptosis via caspase-dependent and caspase-independent pathways in mesenchymal stem cells derived from human adipose tissue, Arch. Toxicol. 85 (2011) 1057–1065.

[78] V. D'Aleo, S. Del Guerra, M. Martano, B. Bonamassa, D. Canistro, A. Soleti, L. Valgimigli, M. Paolini, F. Filipponi, U. Boggi, S. Del Prato, R. Lupi, The non-peptidyl low molecular weight radical scavenger IAC protects human pancreatic islets from lipotoxicity, Mol. Cell. Endocrinol. 309 (2009) 63–66.
[79] S. Piro, M. Anello, C. Di Pietro, M.N. Lizzio, G. Patane, A.M. Rabuazzo, R. Vigneri, M. Purrello, F. Purrello, Chronic exposure to free fatty acids or high glucose induces apoptosis in rat pancreatic islets: possible role of oxidative stress, Metabolism 51 (2002) 1340–1347.
[80] P. Newsholme, E.P. Haber, S.M. Hirabara, E.L. Rebelato, J. Procopio, D. Morgan, H.C. Oliveira-Emilio, A.R. Carpinelli, R. Curi, Diabetes associated cell stress and dysfunction: role of mitochondrial and non-mitochondrial ROS production and activity, J. Physiol. 583 (2007) 9–24.
[81] G. Drews, P. Krippeit-Drews, M. Dufer, Oxidative stress and beta-cell dysfunction, Pflugers Arch. 460 (2010) 703–718.
[82] F. Lang, S. Ullrich, E. Gulbins, Ceramide formation as a target in beta-cell survival and function, Expert Opin. Ther. Targets 15 (2011) 1061–1071.
[83] D. Volonte, F. Galbiati, Caveolin-1, cellular senescence and pulmonary emphysema, Aging (Albany NY) 1 (2009) 831–835.
[84] H. Zou, E. Stoppani, D. Volonte, F. Galbiati, Caveolin-1, cellular senescence and age-related diseases, Mech. Ageing Dev. 132 (2011) 533–542.
[85] A.R. Sanguinetti, H. Cao, C. Corley Mastick, Fyn is required for oxidative- and hyperosmotic-stress-induced tyrosine phosphorylation of caveolin-1, Biochem. J. 376 (2003) 159–168.
[86] A. Wadhawan, C. Smith, R.I. Nicholson, P. Barrett-Lee, S. Hiscox, Src-mediated regulation of homotypic cell adhesion: implications for cancer progression and opportunities for therapeutic intervention, Cancer Treat. Rev. 37 (2011) 234–241.
[87] A. Aleshin, R.S. Finn, SRC: a century of science brought to the clinic, Neoplasia 12 (2010) 599–607.
[88] A. Corcoran, T.G. Cotter, Redox regulation of protein kinases, FEBS J. 280 (2013) 1944–1965.
[89] S.K. Yoo, T.W. Starnes, Q. Deng, A. Huttenlocher, Lyn is a redox sensor that mediates leukocyte wound attraction in vivo, Nature 480 (2011) 109–112.
[90] M. Sverdlov, A.N. Shajahan, R.D. Minshall, Tyrosine phosphorylation-dependence of caveolae-mediated endocytosis, J. Cell. Mol. Med. 11 (2007) 1239–1250.
[91] H. Cao, A.R. Sanguinetti, C.C. Mastick, Oxidative stress activates both Src-kinases and their negative regulator Csk and induces phosphorylation of two targeting proteins for Csk: caveolin-1 and paxillin, Exp. Cell Res. 294 (2004) 159–171.
[92] A.N. Shajahan, Z.C. Dobbin, F.E. Hickman, S. Dakshanamurthy, R. Clarke, Tyrosine phosphorylated caveolin-1 (Y14) increases sensitivity to paclitaxel by inhibiting BCL2 and BCLxL via JNK, J. Biol. Chem. 287 (21) (2012) 17682–17692.
[93] E.M. Khan, J.M. Heidinger, M. Levy, M.P. Lisanti, T. Ravid, T. Goldkorn, Epidermal growth factor receptor exposed to oxidative stress undergoes Src- and caveolin-1-dependent perinuclear trafficking, J. Biol. Chem. 281 (2006) 14486–14493.
[94] A.N. Shajahan, Z.C. Dobbin, F.E. Hickman, S. Dakshanamurthy, R. Clarke, Tyrosine-phosphorylated caveolin-1 (Tyr-14) increases sensitivity to paclitaxel by inhibiting BCL2 and BCLxL proteins via c-Jun N-terminal kinase (JNK), J. Biol. Chem. 287 (2012) 17682–17692.
[95] D. Volonte, B. Kahkonen, S. Shapiro, Y. Di, F. Galbiati, Caveolin-1 expression is required for the development of pulmonary emphysema through activation of the ATM–p53–p21 pathway, J. Biol. Chem. 284 (2009) 5462–5466.
[96] M. Zhang, S.J. Lee, C. An, J.F. Xu, B. Joshi, I.R. Nabi, A.M. Choi, Y. Jin, Caveolin-1 mediates Fas-BID signaling in hyperoxia-induced apoptosis, Free Radic. Biol. Med. 50 (2011) 1252–1262.